Electronic supplementary information

Mechanistic studies of isomeric [2]rotaxanes consisting of two different tetrathiafulvalene units reveal that the movement of cyclobis(paraquat-*p*-phenylene) can be controlled

Sofie K. Jensen, Mathias S. Neumann, Rikke Frederiksen, Mathias L. Skavenborg, Mads C. Larsen, Stinne E. Wessel and Jan O. Jeppesen*

Department of Physics, Chemistry and Pharmacy, University of Southern Denmark, Campusvej 55, 5230 Odense M, Denmark. E-mail: joj@sdu.dk

Table of contents

1 Complexation of TTF derivatives by CBPQT^{4+}

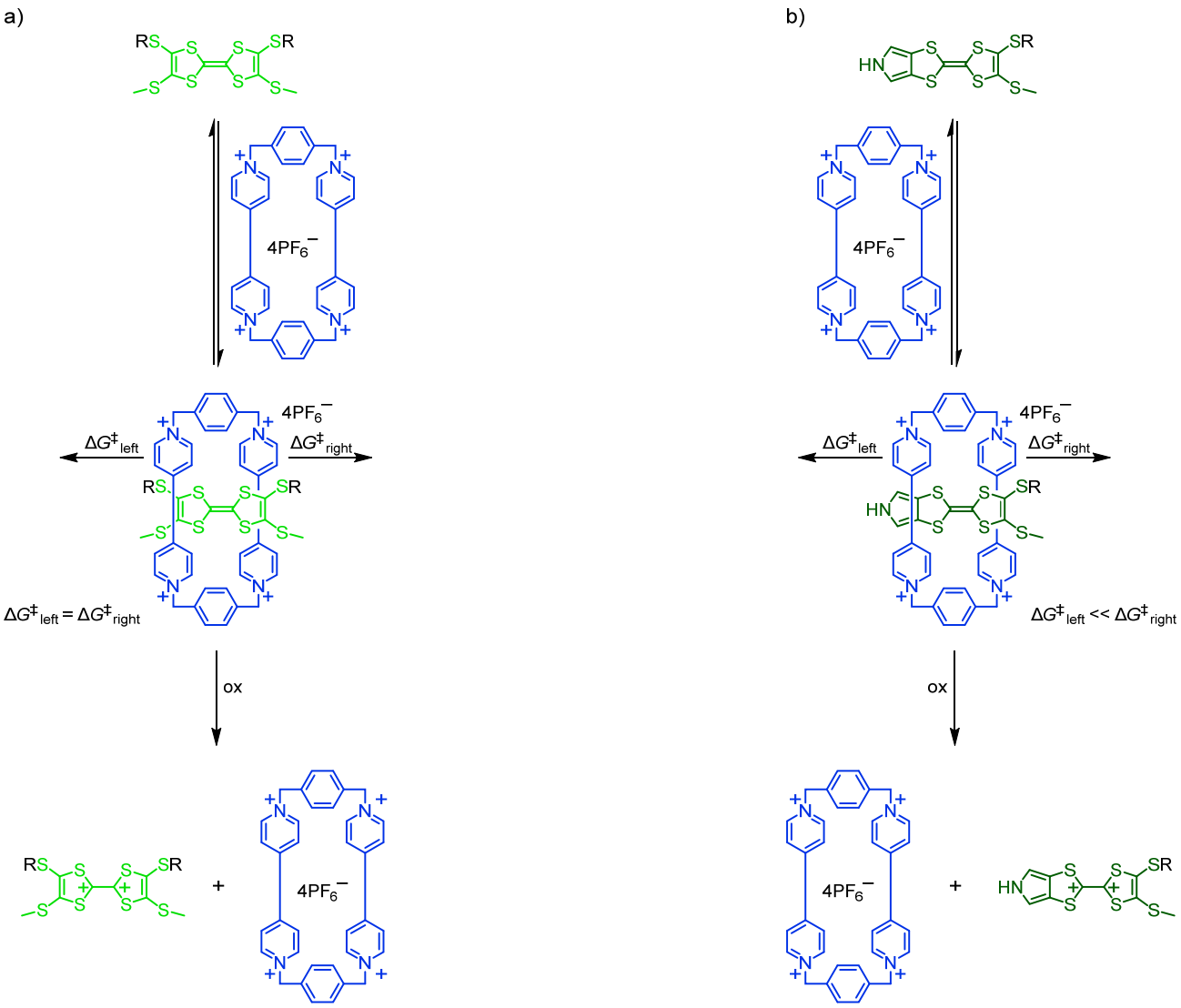

Scheme S1 Complexation of TTF derivatives by CBPQT^{4+} and their decomplexation induced by oxidation of the TTF unit for a) a symmetric TTF unit and b) a non-symmetric MPTTF unit.

2 Experimental details

2.1 General methods

All reactions were performed under an inert atmosphere of N_2 unless otherwise stated. CH_2Cl_2 was distilled before use. DMF and MeCN were dried over molecular sieves (4 Å), while THF and MeOH were dried over molecular sieves (4 Å) and Mg, respectively, and distilled immediately before use. All chemicals were purchased from Sigma Aldrich and were used as received, unless otherwise stated. 2-[4-(2-Cyanoethylthio)-5-ethylthio-1,3-dithiole-2-yliden]-5-tosyl-(1,3)-dithiolo[4,5-*c*]pyrrole[S1] (**3**), 2-(2-(2-(2-bromoethoxy)ethoxy)ethoxy)-1,3-diisopropylbenzene[S2] (**4**), 1,2-bis(iodoethoxy)-ethane[S3] (**7**), 4-(2-cyanoethylthio)-5-methylthio-1,3-dithiole-2-thione[S4] (**9**), 2-(2-(2-[4-(tris(4-*t*-butyl-phenyl)methyl)phenoxy]ethoxy)ethoxy)ethyliodide[S5] (**10**), 4-(2-cyanoethylthio)-5-methylthio-1,3-dithiol-2-one[S4] (**12**), 1,1'-[1,4-phenylene-bis(methylene)]bis(4,4'-bipyridinium)bis(hexafluoro-phosphate)[S6] (**15**•2PF_6), MPTTF derivattive[S2] **17**, and 4-(2-cyanoethylthio)-5-ethylthio-1,3-dithiole-2-thione[S7] (**20**) were all synthesised according to literature procedures. High pressure reactions were performed in a custom made teflon-tube, using a Psika high pressure apparatus. Thin-layer chromatography (TLC) was carried out using aluminium sheets precoated with SiO_2 (Merck 60 F254) and visualised with UV light (254 nm) or I_2 vapour. Column chromatography was carried out using SiO_2 (Merck 60 F 0.040–0.063 mm). ^{1}H NMR and ^{13}C NMR spectra were recorded at 298 K (unless otherwise stated) at 400 MHz/500 MHz and 100 MHz/125 MHz, respectively, on a 400 MHz Bruker AVANCE III spectrometer or a 500 MHz JEOL JNM-ECZR spectrometer, while ^{1}H NMR spectra below 298 K were recorded on a 600 MHz Agilent PremiumCompact+ spectrometer using residual non-deuterated solvent as the internal standard. The solvent signals were assigned according to Fulmer *et al.*[S8] All chemical shifts are quoted on a *δ* scale. The following abbreviations are used in listing the NMR spectra: s = singlet, bs = broad singlet, d = doublet, t = triplet, q = quartet, sept = septet and m = multiplet. Melting points were measured on a Büchi 353 melting point apparatus and are uncorrected. Electrospray ionisation mass spectrometry (ESI-MS) was performed on a Bruker Avance III Daltonics MicrOTOF-Q II ESI-Qq-TOF mass spectrometer. UV-Vis-NIR spectroscopic data were recorded on a Shimadzu UV-1601PC spectrophotometer or an Agilent Cary 5000 spectrophotometer. Cyclic voltammetry (CV) was carried out on an Autolab PGSTAT30 potentiostat. The CV cell consisted of a glassy carbon working electrode (WE), a Pt wire counter electrode (CE) and an $Ag/AgNO_3$ reference electrode (RE). The measurements were carried out in MeCN with *n*-Bu_4N•PF_6 (0.1 M) as the electrolyte and with a scan rate of 100 mV s^{-1} at 298 K. The WE was polished with an Al_2O_3 slurry prior to use and all solutions were degassed (N_2) prior to use. All redox potentials were measured against Ag/Ag^+ and converted into *vs.* ferrocene/ferrocenium (Fc/Fc^+). Elemental analyses were performed by Atlantic Microlabs, Inc., Norcross, GA, USA.

2.2 Synthesis of [2]rotaxane 1•4PF$_6$

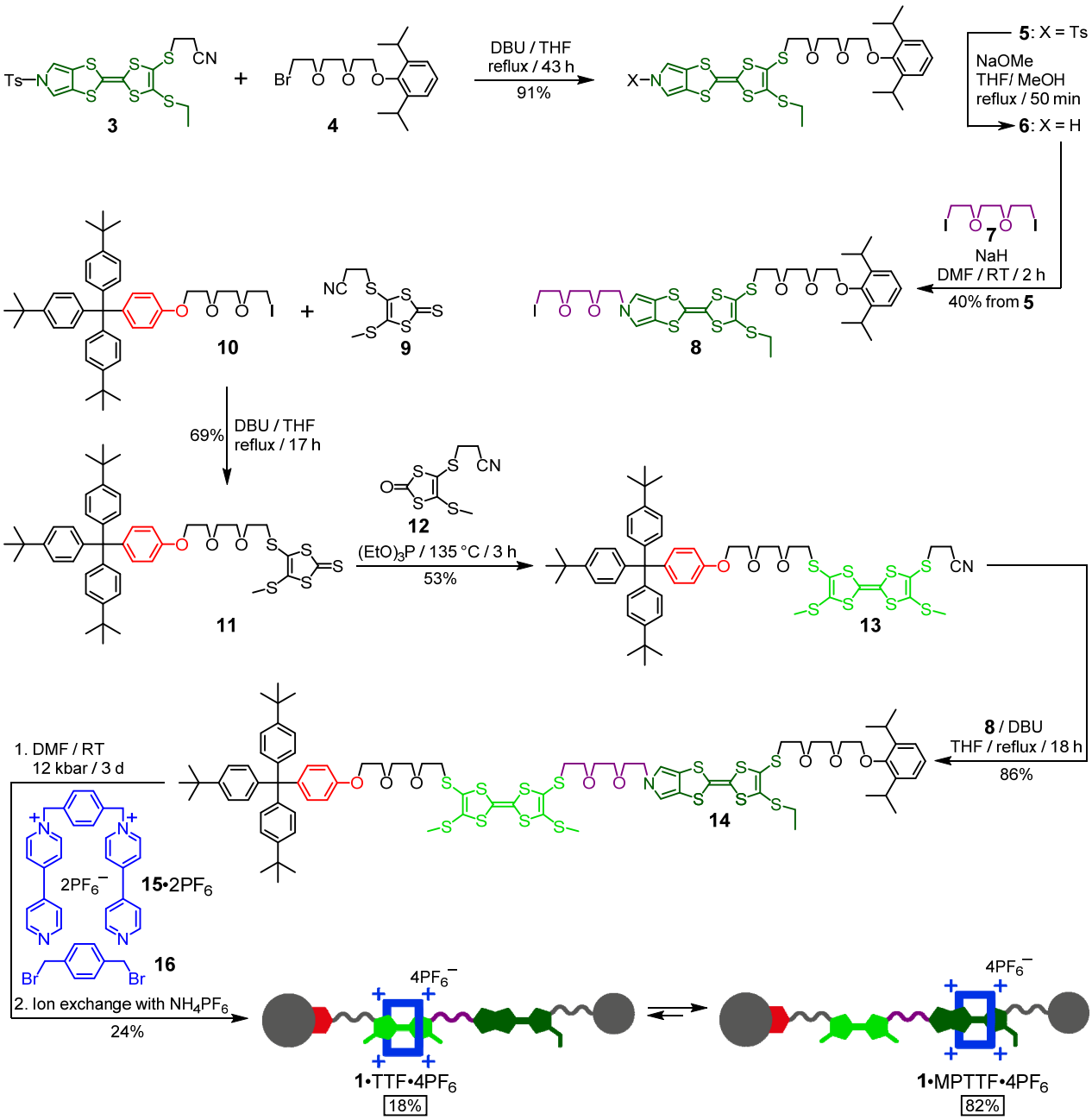

Scheme S2 Synthesis of the dumbbell **14** and the [2]rotaxane **1**•4PF$_6$.

MPTTF derivative 5

2-[4-(2-Cyanoethylthio)-5-ethylthio-1,3-dithiole-2-yliden]-5-tosyl-(1,3)-dithiolo[4,5-*c*]pyrrole (**3**) (497 mg, 0.915 mmol) and 2-(2-(2-(2-bromoethoxy)ethoxy)ethoxy)-1,3-diisopropylbenzene (**4**) (308 mg, 0.824 mmol) were dissolved in anhydrous THF (70 mL) and degassed (N_2, 20 min) before DBU (285 mg, 1.87 mmol) was added. The yellow reaction mixture was heated under reflux for 23 h before another portion of DBU (285 mg, 1.87 mmol) was added. The reaction mixture was heated under reflux for another 20 h and cooled to room temperature before the solvent was removed. The

brown residue was purified by column chromatography (275 mL SiO_2, 5.5 cm Ø, CH_2Cl_2:petroleum ether (bp. 60–80 °C) 4:1). The orange band (R_f = 0.4) was collected, and the solvent evaporated which yielded compound **5** as an orange oil (588 mg, 91%). ^{1}H NMR ($CDCl_3$, 400 MHz): ^{1}H NMR ($CDCl_3$, 400 MHz): δ (ppm) = 1.21 (d, J = 6.9 Hz, 12H), 1.29 (t, J = 7.4 Hz, 3H), 2.41 (s, 3H), 2.84 (q, J = 7.4 Hz, 2H), 3.01 (t, J = 6.7 Hz, 2H), 3.37 (sept, J = 6.9 Hz, 2H), 3.66–3.73 (m, 4H), 3.73–3.78 (m, 2H), 3.83–3.87 (m, 2H), 3.89–3.93 (m, 2H), 6.92 and 6.93 (AB, J_{AB} = 2.1 Hz, 2H), 7.09 (s, 3H), 7.29 (d, J = 8.4 Hz, 2H), 7.72 (d, J = 8.4 Hz, 2H). ^{13}C NMR ($CDCl_3$, 100 MHz): δ (ppm) = 23.1, 25.3, 29.5, 69.1, 69.6, 69.7, 69.9, 72.9, 110.3, 123.0, 126.0, 129.1, 140.8.[S9] MS (ESI): m/z = 782 [M+H]$^+$, 799 [M+NH$_4$]$^+$, 804 [M+Na]$^+$. MS (HiRes-FT ESI) calcd. for $C_{35}H_{43}NNaO_5S_7^+$: 804.1078; found: 804.1115. Anal. calcd. for $C_{35}H_{43}NO_5S_7$: C, 53.75; H, 5.54; N, 1.79; S, 28.69; found: C, 53.62; H, 5.70; N, 1.82; S, 28.83.

MPTTF derivative 8

Compound **5** (577 mg, 0.737 mmol) was dissolved in anhydrous THF:MeOH (100 mL, 1:1, v/v), and the yellow solution was degassed (N_2, 25 min). A solution of NaOMe in MeOH (25% w/w 1.6 mL, 7.0 mmol) was added in one portion and the solution was heated under reflux for 50 min, whereupon the reaction mixture was cooled to room temperature followed by removal of the solvent. The brown residue was re-dissolved in CH_2Cl_2 (75 mL), washed with brine (100 mL) and H_2O (3 × 100 mL), whereafter the organic phase was dried ($MgSO_4$). Removal of the solvent gave compound **6** as a brown oily residue which was used immediately in the next step without any further purification. Compound **6** and 1,2-bis(2-iodoethoxy)ethane (**7**) (2.82 g, 7.63 mmol) were dissolved in anhydrous DMF (150 mL) and degassed (N_2, 30 min) before NaH (60% w/w dispersion in mineral oil, 311 mg, 7.78 mmol) was added in one portion. The orange reaction mixture was stirred at room temperature for 2 h, before the reaction was quenched by dropwise addition of H_2O (50 mL) until the evolution of gas stopped. The solvent was removed, and the resulting brown oil was purified by column chromatography (275 mL SiO_2, 5.5 cm Ø, CH_2Cl_2). The yellow band (R_f = 0.1) was collected, and the solvent evaporated to give compound **8** as a yellow oil (254 mg, 40% from **5**). ^{1}H NMR ($CDCl_3$, 400 MHz): δ (ppm) =1.22 (d, J = 6.9 Hz, 12H), 1.31 (t, J = 7.4 Hz, 3H), 2.86 (q, J = 7.4 Hz, 2H), 3.03 (t, J = 6.8 Hz, 2H), 3.24 (t, J = 6.7 Hz, 2H), 3.38 (sept, J = 6.9 Hz, 2H), 3.55–3.63 (m, 4H), 3.67–3.79 (m, 10H), 3.84–3.93 (m, 4H), 3.95–4.01 (m, 2H), 6.53 and 6.54 (AB, J_{AB} = 2.1 Hz, 2H), 7.09 (s, 3H). ^{13}C NMR ($CDCl_3$, 100 MHz): δ (ppm) = 24.3, 26.4, 70.3, 70.4, 70.8, 70.9, 72.1, 74.0, 124.1.[S9] MS (ESI): m/z = 869 [M]$^+$, 892 [M+Na]$^+$. MS (HiRes-FT ESI) calcd. for $C_{34}H_{48}INO_5S_6^+$: 869.0895; found: 869.0902. Anal. calcd. for $C_{34}H_{48}INO_5S_6$: C, 46.94; H, 5.56; N, 1.61; S, 22.11; found: C, 46.57; H, 5.51; N, 1.50; S, 21.73.

Thione derivative 11

Thione **9** (749 mg, 2.82 mmol) and 2-(2-(2-[4-(tris(4-*t*-butylphenyl)methyl)phenoxy]ethoxy)-ethoxy)ethyliodide (**10**) (1.91 g, 2.56 mmol) were dissolved in anhydrous THF (100 mL) and degassed (N_2, 30 min) before DBU (853 mg, 5.53 mmol) was added in one portion. The reaction mixture was heated under reflux for 18 h, whereupon the solvent was removed. The oily residue was purified by column chromatography (300 mL SiO_2, 6 cm Ø, CH_2Cl_2) and the yellow band (R_f = 0.3) was collected, whereafter the solvent was evaporated providing compound **11** as a yellow solid (1.46 g, 69%). Mp 169.4–171.0 °C. ^{1}H NMR ($CDCl_3$, 400 MHz): δ (ppm) = 1.30 (s, 27H), 2.47 (s,

3H), 3.05 (t, *J* = 6.3 Hz, 2H), 3.64–3.68 (m, 2H), 3.70–3.74 (m, 4H), 3.82–3.87 (m, 2H), 4.08–4.12 (m, 2H), 6.78 (d, *J* = 8.9 Hz, 2H) 7.04–7.10 (m, 8H), 7.23 (d, *J* = 8.6 Hz, 6H). ^{13}C NMR ($CDCl_3$, 100 MHz): *δ* (ppm) = 19.3, 31.5, 34.5, 36.4, 63.3, 67.5, 70.1, 70.2, 70.9, 71.0, 77.4, 113.3, 124.2, 130.9, 132.4, 140.0, 144.3, 148.5, 156.7, 211.1.[S9] MS (ESI): *m*/*z* = 831 [*M*+H]$^+$, 853 [*M*+Na]$^+$. MS (HiRes-FT ESI) calcd. for $C_{47}H_{58}NaO_3S_5^+$: 853.2882; found: 853.2894. Anal. calcd. for $C_{47}H_{58}O_3S_5$: C, 67.91; H, 7.03; S, 19.28; found: C, 68.20; H, 7.11; S, 18.99.

TTF derivative 13

Thione **11** (3.50 g 13.1 mmol) and 4-(2-cyanoethylthio)-5-methylthio-1,3-dithiol-2-one (**12**), (2.75 g, 8.83 mmol) were suspended in distilled $(EtO)_3P$ (75 mL) and heated to 130 °C. Two additional portions of the thione **11** were added after 9 min (1.10 g, 4.15 mmol) and 18 min (1.09 g, 4.13 mmol), respectively. The orange reaction mixture was stirred for 3 h at 130 °C and cooled to room temperature, whereupon cold MeOH (100 mL) was added. The reaction mixture was left in the freezer for 24 h and the resulting precipitate was collected by filtration and washed with MeOH. The orange solid was re-dissolved in CH_2Cl_2 (500 mL) and Celite 545 (50 mL) was added to the orange solution. Removal of the solvent gave an orange residue which was purified by column chromatography (800 mL SiO_2, 8 cm Ø, petroleum ether (bp. 60–80 °C):CH_2Cl_2 1:3). The orange band (R_f = 0.3) was collected and concentrated to give an orange solid (2.89 g, 53%) containing compound **13** as a mixture of *E*- and *Z*-isomers. The data given below are for a mixture of the *E*- and *Z*-isomers. Mp 148.3–150.0 °C. ^{1}H NMR ($CDCl_3$, 400 MHz): *δ* (ppm) = 1.30 (s, 27H), 2.41, 2.41, 2.45 and 2.46 (4 × s, 6H), 2.68 and 2.69 (2 × t, *J* = 7.3 Hz, 2H), 2.96–3.04 (m, 4H), 3.65–3.75 (m, 6H), 3.83–3.87 (m, 2H), 4.06–4.14 (m, 2H), 6.77 (d, *J* = 8.8 Hz, 2H), 7.04–7.10 (m, 8H), 7.20–7.25 (m, 6H). ^{13}C NMR ($CDCl_3$, 100 MHz): *δ* (ppm) = 19.0, 19.3, 31.6, 34.5, 35.7, 63.2, 67.5, 70.1, 70.8, 71.0, 77.4, 113.2, 124.1, 130.9, 132.4, 144.3, 148.5, 156.7.[S9] MS (ESI): *m*/*z* = 1031 [*M*]$^+$. MS (HiRes-FT ESI) calcd. for $C_{54}H_{65}NO_3S_8^+$: 1031.2725; found: 1031.2558. Anal. calcd. for $C_{54}H_{65}NO_3S_8$: C, 62.81; H, 6.35; N, 1.36; S, 24.84; found: C, 62.64; H, 6.39; N, 1.37; S, 24.62.

Dumbbell 14

TTF derivative **13** (251 mg, 0.243 mmol) and MPTTF derivative **8** (199 mg, 0.229 mmol) were dissolved in anhydrous THF (50 mL) and degassed (N_2, 20 min) before DBU (81 mg, 0.54 mmol) was added in one portion. The reaction mixture was heated under reflux for 18 h and cooled to room temperature. The solvent was removed, and the resulting dark residue was purified by gradient column chromatography (150 mL SiO_2, 4 cm Ø, CH_2Cl_2:EtOAc 1:0–20:1). The yellow band (R_f = 0.2, CH_2Cl_2) was collected and evaporated which gave a yellow solid (340 mg, 86%) containing compound **14** as a mixture of *E*- and *Z*-isomers and traces of grease. The data given below are for a mixture of the *E*- and *Z*-isomers. Mp 106.2–108.7 °C. ^{1}H NMR (CD_3CN, 400 MHz): *δ* (ppm) = 1.17 and 1.18 (2 × d, *J* = 6.9 Hz ,12H), 1.25 (t, *J* = 7.3 Hz, 3H), 1.28 (s, 27H), 2.35, 2.36 and 2.38 (3 × s, 6H), 2.85 (q, *J* = 7.3 Hz, 2H), 2.88–2.96 (m, 4H), 3.01 (t, *J* = 6.6 Hz, 2H), 3.38 (sept, *J* = 6.9 Hz, 2H), 3.48–3.51 (m, 4H), 3.51–3.57 (m, 4H), 3.57–3.69 (m, 12H), 3.71–3.77 (m, 4H), 3.82–3.85 (m, 2H), 3.93–3.98 (m, 2H), 4.04–4.08 (m, 2H), 6.63 and 6.64 (AB, J_{AB} = 2.3 Hz, 2H), 6.78–6.82 (m, 2H), 7.03–7.18 (m, 11H), 7.28–7.32 (m, 6H). ^{13}C NMR ($CDCl_3$, 125 MHz): *δ* (ppm) = 15.2, 19.2, 19.27, 19.28, 24.3, 26.4, 30.6, 31.5, 34.4, 35.6, 35.73, 35.75, 50.8, 63.2, 67.4, 70.0, 70.2, 70.2, 70.2, 70.3, 70.7, 70.8, 70.8, 70.8, 70.8, 70.9, 70.9, 71.0, 71.3, 71.3, 113.1, 113.2, 113.2, 119.0, 124.1, 124.2,

124.7, 128.7, 130.9, 130.9, 132.4, 139.9, 142.0, 144.3, 148.5, 153.2, 156.7.[S9] MS (ESI): *m*/*z* = 1719 [M^+]. MS (HiRes-FT ESI) calcd. for $C_{85}H_{109}NO_8S_{14}^+$: 1719.4238; found: 1719.3951. Anal. calcd. for $C_{85}H_{109}NO_8S_{14}$: C, 59.30; H, 6.38; N, 0.81; S, 26.07. Anal. calcd. for $C_{85}H_{109}NO_8S_{14} + 2CH_2$: C, 59.72; H, 6.51; N, 0.80; S, 25.65; found: C, 59.73; H, 6.14; N, 0.93; S, 25.21.

[2]Rotaxane 1•4PF$_6$

A mixture of 1,1'-[1,4-phenylene-bis(methylene)]bis(4,4'-bipyridinium)-bis(hexafluorophosphate) (**15**•2PF$_6$) (183 mg, 0.258 mmol) and 1,4-bis(bromomethyl)benzene (**16**) (73.0 mg, 0.277 mmol) were transferred to a teflon-tube, where after a solution of the dumbbell **14** (111 mg, 0.0645 mmol) in anhydrous DMF (1.9 mL) was added. The teflon-tube was sealed and subjected to 12 kbar pressure at room temperature for 3 d. The green reaction mixture was directly subjected to column chromatography (200 mL SiO_2, 4 cm Ø, Me_2CO:NH_4PF_6 1:0–100:0.25 (v/w)). Unreacted dumbbell **14** was eluted with Me_2CO, whereupon the eluent was changed to Me_2CO:NH_4PF_6 100:0.25 (v/w) and the green band containing **1**•4PF$_6$ was collected and concentrated to a minimum volume. Addition of cold H_2O (75 mL, 5 °C) gave a green precipitate which was collected by filtration, washed with H_2O (3 × 2 mL) and Et_2O (3 × 2 mL) and dried affording a green solid (44.3 mg, 24%) containing a mixture of the two translational isomers of **1**•4PF$_6$; each as a mixture of *E*- and *Z*-isomers. The data given below are for a mixture of the two translational isomers. Mp 135.3–138.9 °C. MS (ESI): *m*/*z* = 795 [M−3PF$_6$]$^{3+}$, 1265 [M−2PF$_6$]$^{2+}$. MS (HiRes-FT ESI) calcd. for $C_{121}H_{141}F_6N_5O_8PS_{14}^{3+}$: 794.8832; found: 794.8836. Anal. calcd. for $C_{121}H_{141}F_{24}N_5O_8P_4S_{14}$: C, 51.50; H, 5.04; N, 2.48; S, 15.90. Anal. calcd. for $C_{121}H_{141}F_{24}N_5O_8P_4S_{14} + H_2O$: C, 51.17; H, 5.08; N, 2.47; S, 15.80; found: C, 51.00; H, 5.18; N, 2.61; S, 16.35.

Data for **1**•MPTTF•4PF$_6$: ^{1}H NMR (CD_3CN, 400 MHz): δ (ppm) = 1.17 (d, J = 6.9 Hz, 12H), 1.28 (s, 27H), 1.52 (t, J = 7.4 Hz, 3H), 2.31, 2.32, 2.37 and 2.38 (4 × s, 6H), 2.76 and 2.77 (2 × t, J = 6.2 Hz, 2H), 2.96 and 2.97 (2 × t, J = 6.2 Hz, 2H), 3.11 (q, J = 7.4 Hz, 2H), 3.30 (t, J = 6.3 Hz, 2H), 3.32–3.40 (m, 2H), 3.50–3.67 (m, 8H), 3.67–3.76 (m, 4H), 3.76–3.89 (m, 12H), 3.89–3.96 (m, 4H), 4.03–4.10 (m, 2H), 5.67–5.79 (m, 8H), 6.11 and 6.14 (AB, J_{AB} = 1.7 Hz, 2H), 6.78–6.83 (m, 2H), 7.04–7.18 (m, 11H), 7.26–7.34 (m, 6H), 7.66–7.81 (m, 12H), 7.93–8.07 (m, 4H), 8.76–9.12 (m, 8H). ^{13}C NMR (CD_3CN, 125 MHz): δ (ppm) = 15.8, 19.2, 19.27, 19.33, 24.35, 24.39, 26.9, 27.0, 30.8, 31.2, 31.5, 34.9, 36.3, 36.4, 64.0, 68.3, 70.2, 70.30, 70.32, 70.5, 70.6, 70.7, 70.9, 71.1, 71.11, 71.11, 71.2, 71.2, 71.3, 71.3, 71.4, 71.4, 71.4, 110.2, 114.4, 116.9, 117.1, 125.0, 125.1, 125.4, 125.8, 131.2, 131.2, 131.7, 131.7, 132.7, 132.7, 137.5, 137.5, 142.7, 145.5, 147.1, 149.4, 153.9, 157.6.[S9]

2.3 Synthesis of [2]rotaxane 2•4PF$_6$

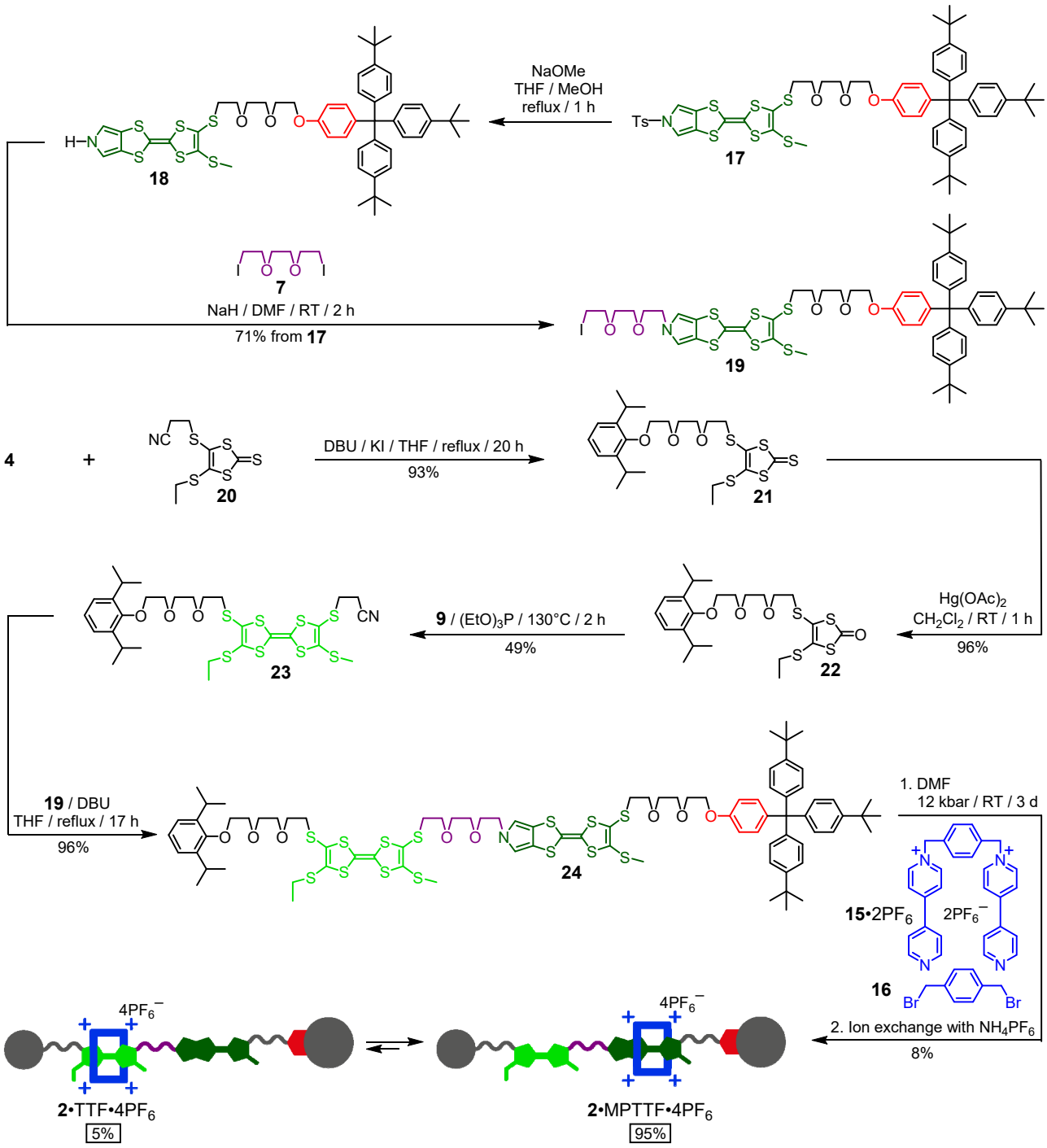

Scheme S3 Synthesis of the dumbbell **24** and the [2]rotaxane **2**•4PF$_6$.

MPTTF derivative 19

Compound **17** (802 mg, 0.732 mmol) was dissolved in anhydrous THF:MeOH (125 mL, 1:1, v/v), and the yellow solution was degassed (N_2, 20 min). A solution of NaOMe (25% w/w in MeOH, 1.6 mL, 7.00 mmol) was added in one portion and the reaction mixture was heated under reflux for 1 h,

whereafter it was cooled to room temperature followed by removal of the solvent. The yellow residue was re-dissolved in CH_2Cl_2 (100 mL), washed with brine (200 mL) and H_2O (2 × 100 mL) before being dried ($MgSO_4$). Removal of the solvent gave compound **18** as an orange oily residue which was used immediately in the next step without any further purification. Compound **18** and 1,2-bis(2-iodoethoxy)ethane (**7**) (3.25 g, 8.78 mmol) were dissolved in anhydrous DMF (200 mL) and degassed (N_2, 30 min) before NaH (60% w/w dispersion in mineral oil, 271 mg, 6.78 mmol) was added in one portion. The yellow reaction mixture was stirred at room temperature for 2 h before the reaction was stopped by dropwise addition of H_2O (100 mL) until the evolution of gas stopped. The solvent was removed, and the orange semisolid was re-dissolved in CH_2Cl_2 (100 mL), washed with brine (3 × 150 mL), H_2O (2 × 100 mL) and dried ($MgSO_4$). Removal of the solvent gave a brown solid, which was purified by column chromatography (350 mL SiO_2, 6 cm Ø, CH_2Cl_2). The yellow band (R_f = 0.4) was collected, and the solvent evaporated to provide compound **19** as a yellow solid (615 mg, 71% from **17**). Mp 130.0–132.5°C. ^{1}H NMR ($CDCl_3$, 400 MHz): δ (ppm) = 1.30 (s, 27H), 2.40 (s, 3H), 3.00 (t, J = 6.7 Hz, 2H), 3.24 (t, J = 6.6 Hz, 2H), 3.55–3.62 (m, 4H), 3.64–3.73 (m, 10H), 3.82–3.85 (m, 2H), 3.94–3.98 (m, 2H), 4.07–4.10 (m, 2H), 6.51 and 6.52 (AB, J = 2.1 Hz, 2H), 6.76 (d, J = 8.8 Hz, 2H), 7.04–7.10 (m, 8H), 7.20–7.25 (m, 6H). ^{13}C NMR ($CDCl_3$, 100 MHz): δ (ppm) = 3.07, 19.2, 31.6, 34.5, 35.6, 63.3, 67.5, 70.1, 70.3, 70.4, 70.8, 70.9, 70.9, 72.1, 77.4, 113.3, 119.1, 119.1, 124.2, 130.6, 130.9, 132.4, 139.9, 144.3, 148.5, 156.8.[S9] MS (ESI): m/z = 1181 $[M]^+$. MS (HiRes-FT ESI) calcd. for $C_{58}H_{72}INO_5S_6^+$: 1181.2774; found: 1181.2715. Anal. calcd. for $C_{58}H_{72}INO_5S_6$: C, 58.91; H, 6.14; N, 1.18; S, 16.27; found: C, 59.05; H, 6.13; N, 1.21; S, 16.34.

Thione derivative 21

2-(2-(2-(2-Bromoethoxy)ethoxy)ethoxy)-1,3-diisopropylbenzene (**4**) (2.49 g, 6.67 mmol), thione **20** (2.00 g, 7.16 mmol) and KI (331 mg, 2.00 mmol) were dissolved in anhydrous THF (250 mL) and degassed (N_2, 20 min), before DBU (2.15 g, 14.1 mmol) was added in one portion. The reaction mixture was heated under reflux for 20 h, whereafter the solvent was removed. The brown oily residue was dissolved in CH_2Cl_2 (250 mL) and washed with H_2O (3 × 250 mL). The combined aqueous phases were extracted with CH_2Cl_2 (100 mL), and the combined organic phases were dried ($MgSO_4$) followed by removal of the solvent. The brown oily residue was purified by column chromatography (600 mL SiO_2, 8 cm Ø, CH_2Cl_2:EtOAc 49:1) and the orange band (R_f = 0.6) was collected. Removal of the solvent gave compound **21** as an orange oil (3.20 g, 93%). ^{1}H NMR ($CDCl_3$, 400 MHz): δ (ppm) = 1.22 (d, J = 6.9 Hz, 12H), 1.36 (t, J = 7.4 Hz, 3H), 2.92 (q, J = 7.4 Hz, 2H), 3.09 (t, J = 6.4 Hz, 2H), 3.38 (sept, J = 6.9 Hz, 2H), 3.68–3.73 (m, 2H), 3.74–3.79 (m, 4H), 3.84–3.88 (m, 2H), 3.90–3.94 (m, 2H), 7.10 (s, 3H). ^{13}C NMR ($CDCl_3$, 100 MHz): δ (ppm) = 15.1, 24.3, 26.4, 31.1, 36.4, 70.1, 70.8, 70.9, 71.1, 74.0, 124.1, 124.8, 135.3, 137.8, 141.9, 153.2, 211.4. MS (ESI): m/z = 519 $[M+H]^+$, 536 $[M+NH_4]^+$, 541 $[M+Na]^+$. MS (HiRes-FT ESI) calcd. for $C_{23}H_{34}NaO_3S_5^+$: 541.1004; found: 541.1018. Anal. calcd. for $C_{23}H_{34}O_3S_5$: C, 53.25; H, 6.61; S, 30.90; found: C, 53.37; H, 6.44; S, 31.09.

Ketone derivative 22

Compound **21** (3.11 g, 5.99 mmol) was dissolved in CH_2Cl_2 (125 mL) and $Hg(OAc)_2$ (6.11 g, 19.2 mmol) was added. The resulting orange suspension was stirred at room temperature for 1 h during which it gradually became lighter yellow. The reaction mixture was filtered through a pad of

Celite 545 (125 mL, 8 cm Ø), whereafter the resulting solid on top of the Celite was washed with CH_2Cl_2 (6 × 50 mL). The combined filtrate was washed with H_2O (2 × 300 mL) and dried ($MgSO_4$) before the solvent was removed. The yellow oily residue was purified by column chromatography (300 mL SiO_2, 6 cm Ø, CH_2Cl_2). The pale yellow band (R_f = 0.5) was collected giving compound **22** as a pale yellow oil (2.90 g, 96%). ^{1}H NMR ($CDCl_3$, 400 MHz): δ (ppm) = 1.22 (d, J = 6.9 Hz, 12H), 1.34 (t, J = 7.4 Hz, 3H), 2.89 (q, J = 7.4 Hz, 2H), 3.07 (t, J = 6.4 Hz, 2H), 3.38 (sept, J = 6.9 Hz, 2H), 3.68–3.78 (m, 6H), 3.84–3.88 (m, 2H), 3.90–3.94 (m, 2H), 7.10 (s, 3H). ^{13}C NMR ($CDCl_3$, 100 MHz): δ (ppm) = 15.1, 24.3, 26.4, 31.0, 36.2, 70.1, 70.8, 70.9, 71.1, 74.0, 124.2, 124.8, 142.0, 153.2.[S9] MS (ESI): m/z = 503 $[M+H]^+$, 520 $[M+NH_4]^+$, 525 $[M+Na]^+$. MS (HiRes-FT ESI) calcd. for $C_{23}H_{34}NaO_4S_4^+$: 525.1232; found: 525.1249. Anal. calcd. for $C_{23}H_{34}O_4S_4$: C, 54.95; H, 6.82; S, 25.51; found: C, 55.14; H, 6.77; S, 25.22.

TTF derivative 23

Compound **22** (2.88 g, 5.73 mmol) and 4-(2-cyanoethylthio)-5-methylthio-1,3-dithiole-2-thione (**9**) (2.28 g, 8.60 mmol) were suspended in distilled $(EtO)_3P$ and heated to 130 °C. Two additional portions of the thione **9** were added after 7 min (762 mg, 2.87 mmol) and after 14 min (762 mg, 2.87 mmol), respectively. The dark orange reaction mixture was stirred for 1.5 h at 130 °C and cooled to room temperature, whereupon the suspension was concentrated. The resulting red semisolid was re-dissolved in CH_2Cl_2 (200 mL), washed with brine (100 mL) and H_2O (2 x 200 mL) and dried ($MgSO_4$) before Celite 545 (75 mL) was added to the organic phase. Removal of the solvent gave an orange semisolid residue which was purified by column chromatography (700 mL SiO_2, 8 cm Ø, petroleum ether (bp. 60–80 °C):EtOAc 2:1). The orange band (R_f = 0.2) was collected and concentrated to give a red sticky solid (2.00 g, 49%) containing compound **23** as a mixture of *E*- and *Z*-isomers. The data given below are for a mixture of the *E*- and *Z*-isomers. ^{1}H NMR ($CDCl_3$, 400 MHz): δ (ppm) = 1.22 (d, J = 6.9 Hz, 12H), 1.32 (t, J = 7.4 Hz, 3H), 2.46 and 2.47 (2 × s, 3H), 2.69 and 2.70 (2 × t, J = 7.3 Hz, 2H), 2.86 and 2.86 (2 x q, J = 7.4 Hz, 2H), 2.98–3.06 (m, 4H), 3.38 (sept, J = 6.9 Hz, 2H), 3.68–3.79 (m, 6H), 3.84–3.89 (m, 2H), 3.89–3.94 (m, 2H), 7.09 (s, 3H). ^{13}C NMR ($CDCl_3$, 100 MHz): δ (ppm) = 15.2, 18.9, 19.2, 24.3, 26.4, 30.7, 31.4, 35.7, 70.3, 70.3, 70.8, 70.9, 71.1, 71.1, 74.0, 117.7, 124.2, 124.8, 129.0, 142.0, 153.2.[S9] MS (ESI): m/z = 719 $[M]^+$. MS (HiRes-FT ESI) calcd. for $C_{30}H_{41}NO_3S_8^+$: 719.0847; found: 719.0841. Anal. calcd. for $C_{30}H_{41}NO_3S_8$: C, 50.04; H, 5.74; N, 1.95; S, 35.62; found: C, 50.11; H, 5.81; N, 2.03; S, 35.89.

Dumbbell 24

TTF derivative **23** (284 mg, 0.394 mmol) and MPTTF derivative **19** (437 mg, 0.370 mmol) were dissolved in anhydrous THF (50 mL) and degassed (N_2, 35 min) before DBU (0.12 g, 0.79 mmol) was added in one portion. The reaction mixture was heated under reflux for 17 h and cooled to room temperature. The solvent was removed, and the resulting residue was purified by gradient column chromatography (275 mL SiO_2, 5.5 cm Ø, CH_2Cl_2:EtOAc 1:0–20:1). The yellow band (R_f = 0.2, CH_2Cl_2) was collected and evaporated to give a brown solid (610 mg, 96%) containing compound **24** as a mixture of *E*- and *Z*-isomers. The data given below are for a mixture of the *E*- and *Z*-isomers. Mp 101.3–102.6 °C. ^{1}H NMR (CD_3CN, 400 MHz): δ (ppm) = 1.18 and 1.19 (2 × d, J = 6.9 Hz, 12H), 1.23 and 1.24 (2 × t, J = 7.3 Hz, 3H), 1.28 (s, 27H), 2.37, 2.37 and 2.38 (3 × s, 6H), 2.79–2.87 (m, 2H), 2.91 and 2.91 (2 × t, J = 6.2 Hz, 2H), 2.94–3.01 (m, 4H), 3.39 (sept, J = 6.9 Hz, 2H), 3.46–3.67

(m, 20H), 3.71–3.77 (m, 4H), 3.83–3.87 (m, 2H), 3.93 (t, J = 4.8 Hz, 2H), 4.00–4.05 (m, 2H), 6.63 (s, 2H), 6.76–6.81 (m, 2H), 7.07–7.19 (m, 11H), 7.28–7.33 (m, 6H). ^{13}C NMR ($CDCl_3$, 125 MHz): δ (ppm) = 15.3, 19.2, 19.3, 24.3, 26.4, 30.6, 31.5, 34.4, 35.5, 35.7, 35.7, 35.8, 50.8, 63.2, 67.4, 70.0, 70.2, 70.2, 70.2, 70.3, 70.3, 70.7, 70.7, 70.8, 70.8, 70.8, 70.8, 70.9, 71.2, 71.2, 71.3, 74.0, 113.1, 113.2, 113.3, 124.1, 124.2, 124.8, 130.9, 132.4, 139.9, 142.0, 144.3, 148.5, 153.2, 156.8.[S9] MS (ESI): m/z = 1719 $[M]^+$, 1737 $[M+NH_4]^+$, 1742 $[M+Na]^+$. MS (HiRes-FT ESI) calcd. for $C_{85}H_{109}NNaO_8S_{14}^+$: 1742.4135; found: 1742.4198. Anal. calcd. for $C_{85}H_{109}NO_8S_{14}$: C, 59.30; H, 6.38; N, 0.81; S, 26.07; found: C, 59.03; H, 6.43; N, 0.90; S, 25.99.

[2]Rotaxane 2•4PF$_6$

A mixture of 1,1'-[1,4-phenylene-bis(methylene)]bis(4,4'-bipyridinium)-bis(hexafluorophosphate) (**15**•2PF$_6$) (479 mg, 0.678 mmol) and 1,4-bis(bromomethyl)benzene (**16**) (184 mg, 0.697 mmol) were transferred to a teflon-tube, whereupon a solution of the dumbbell **24** (286 mg, 0.166 mmol) in anhydrous DMF (1.7 mL) was added. The teflon-tube was sealed and subjected to 12 kbar pressure at room temperature for 3 d. The resulting green reaction mixture was directly subjected to column chromatography (200 mL SiO_2, 4 cm Ø, Me_2CO:NH_4PF_6 1:0–100:0.25 (v/w)). Unreacted dumbbell **24** was eluted with Me_2CO, whereupon the eluent was changed to Me_2CO:NH_4PF_6 100:0.25 (v/w) and the green band containing **2**•4PF$_6$ was collected and concentrated to a minimum volume. Addition of cold H_2O (50 mL, 5 °C) gave a green precipitate which was collected by filtration, washed with H_2O (3 × 2 mL) and Et_2O (3 × 2 mL) and dried affording a green solid (35.6 mg, 8%) containing a mixture of the two translational isomers of **2**•4PF$_6$; each as a mixture of *E*- and *Z*-isomers. The data given below are for a mixture of the two translational isomers. Mp 152.0–153.2 °C. MS (ESI): m/z = 795 $[M-3PF_6]^{3+}$, 1265 $[M-2PF_6]^{2+}$. MS (HiRes-FT ESI) calcd. for $C_{121}H_{141}F_6N_5O_8PS_{14}^{3+}$: 794.8832; found: 794.8816. Anal. calcd. for $C_{121}H_{141}F_{24}N_5O_8P_4S_{14}$: C, 51.50; H, 5.04; N, 2.48; S, 15.90; found: C, 51.20; H, 5.08; N, 2.60; S, 15.67.

Data for **2**•MPTTF•4PF$_6$: ^{1}H NMR (CD_3CN, 400 MHz): δ (ppm) = 1.17 and 1.17 (2 × d, J = 6.9 Hz, 12H), 1.24 and 1.24 (2 × t, J = 7.3 Hz, 3H) 1.27 (s, 27H), 2.30 and 2.31 (2 × s, 3H), 2.68 (s, 3H), 2.74 and 2.75 (2 × t, J = 6.1 Hz, 2H), 2.83 and 2.85 (2 × q, J = 7.3 Hz, 2H), 3.00 (2 × t, J = 6.1 Hz, 2H), 3.24 (t, J = 6.3 Hz, 2H), 3.33–3.40 (m, 2H), 3.52 and 3.53 (2 × t, J = 6.1 Hz, 2H), 3.59–3.70 (m, 8H), 3.73–3.94 (m, 16H), 4.00–4.04 (m, 2H), 4.06–4.11 (m, 2H), 5.66–5.77 (m, 8H), 6.17 and 6.20 (AB, J_{AB} = 2.0 Hz, 2H) 6.68 (d, J = 8.8 Hz, 2H), 7.04–7.18 (m, 11H), 7.27–7.34 (m, 6H), 7.65–7.81 (m, 12H), 7.93–8.13 (m, 4H), 8.73–9.16 (m, 8H). ^{13}C NMR (CD_3CN, 125 MHz): δ (ppm) = 15.5, 19.2, 19.3, 24.4, 26.9, 30.8, 31.1, 31.1, 31.5, 34.9, 64.0, 65.6, 65.6, 68.2, 70.2, 70.2, 70.6, 70.6, 71.1, 71.2, 71.2, 71.2, 71.3, 71.4, 71.4, 71.4, 71.4, 71.4, 75.0, 108.8, 110.2, 114.2, 116.9, 117.1, 125,0, 125.0, 125.5, 125.7, 125.7, 131.1, 131.2, 131.7, 132.7, 140.8, 142.8, 145.5, 149.5, 157.4.[S9]

2.4 Characterisation of 1•OP^{8+} and 2•OP^{8+}

[2]Rotaxane 1•OP^{8+}

Tris(*p*-bromophenyl)ammoniumyl hexachloroantimonate ($TBPASbCl_6$) (8.7 mg, 10.7 μmol) was added to a solution of the [2]rotaxane **1**•4PF$_6$ (3.05 mg, 1.08 μmol) in CD_3CN (720 μL), whereupon

a ^{1}H NMR spectrum of **1**•OP^{8+} was recorded. ^{1}H NMR (400 MHz, CD_3CN, 298 K): *δ* (ppm) = 1.16 (d, *J* = 6.9 Hz, 12H), 1.37 (s, 27H), 1.40–1.44 (m, 2H), 1.53 (t, *J* = 7.3 Hz, 3H), 2.54 (d, *J* = 8.8 Hz, 2H), 2.94–3.07 (m, 6H), 3.34 (sept, *J* = 6.9 Hz, 2H), 3.40–3.45 (m, 2H), 3.51–3.61 (m, 4H), 3.61−3.69 (m, 6H), 3.69–3.78 (m, 6H), 3.79–3.86 (m, 4H), 3.86–3.93 (m, 4H), 3.93–4.07 (m, 6H), 4.51–4.60 (m, 2H), 5.79 and 5.80 (AB, J_{AB} = 14.1 Hz, 8H), 6.27 (d, *J* = 8.8 Hz, 2H), 7.06–7.14 (m, 3H), 7.35 (d, *J* = 8.5 Hz, 6H), 7.52–7.68 (m, 16H), 8.02 (s, 2H), 8.84 ppm (d, *J* = 6.4 Hz, 8H).

[2]Rotaxane 2•OP^{8+}

Tris(*p*-bromophenyl)ammoniumyl hexachloroantimonate ($TBPASbCl_6$) (8.6 mg, 10.5 μmol) was added to a solution of the [2]rotaxane **2**•4PF_6 (2.97 mg, 1.05 μmol) in CD_3CN (700 μL), whereafter a ^{1}H NMR spectrum of **2**•OP^{8+} was recorded. ^{1}H NMR (400 MHz, CD_3CN, 298 K): *δ* (ppm) = 1.19 (d, *J* = 6.9 Hz, 12H), 1.37 (s, 27H), 1.40–1.44 (m, 2H), 1.51 (t, *J* = 7.3 Hz, 3H), 2.54 (d, *J* = 8.4 Hz, 2H), 3.00 (s, 3H), 3.04 (s, 3H), 3.36 (sept, *J* = 6.9 Hz, 2H), 3.40–3.47 (m, 4H), 3.52–3.58 (m, 2H), 3.58−3.69 (m, 8H), 3.69–3.78 (m, 6H), 3.80–3.93 (m, 8H), 3.93–4.07 (m, 4H), 4.54–4.61 (m, 2H), 5.80 and 5.81 (AB, J_{AB} = 13.8 Hz, 8H), 6.27 (d, *J* = 8.4 Hz, 2H), 7.05–7.15 (m, 3H), 7.35 (d, *J* = 8.4 Hz, 6H), 7.50–7.72 (m, 16H), 8.08 (s, 2H), 8.85 (d, *J* = 6.3 Hz, 8H).

3 ESI mass spectrum of 1•4PF_6

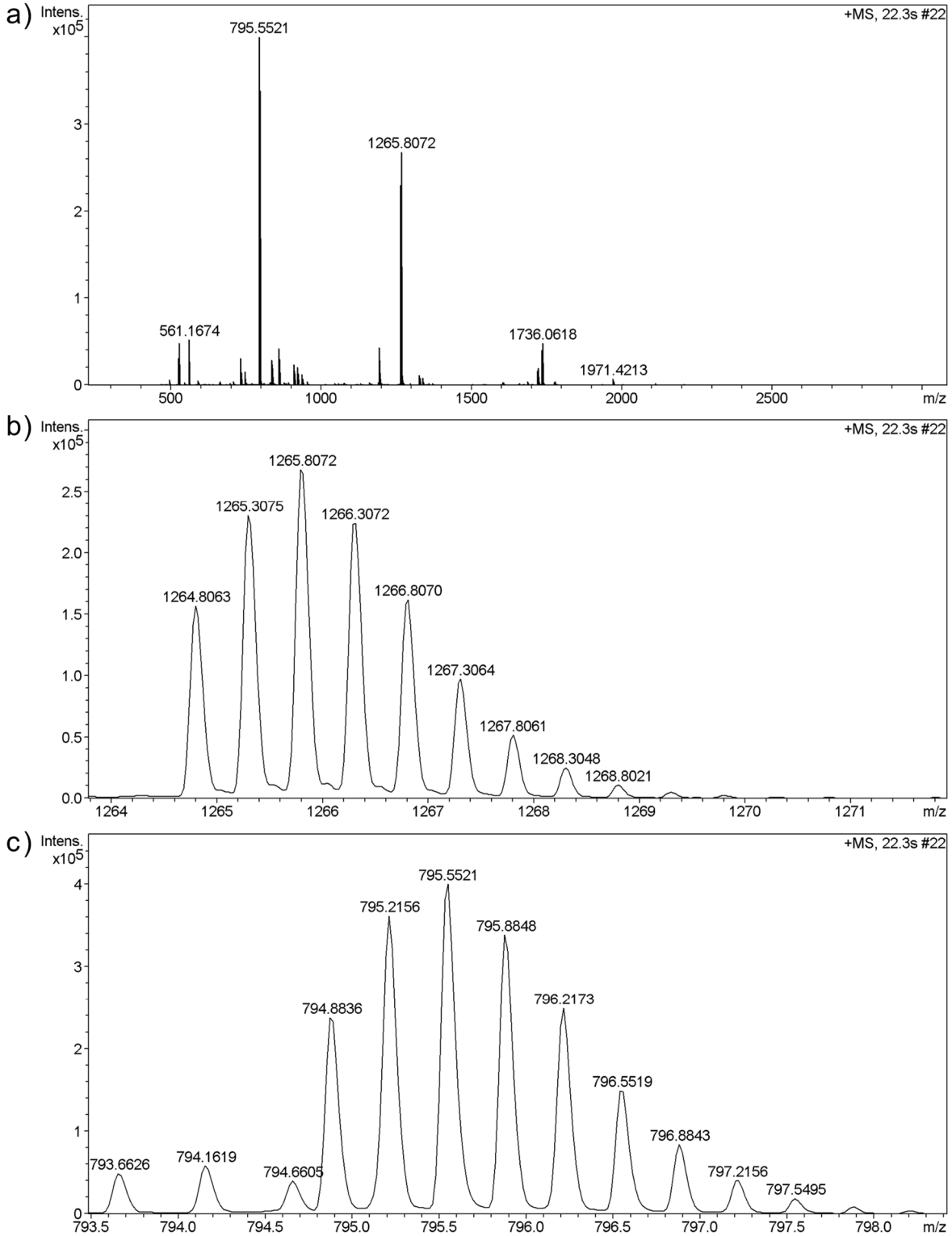

Fig. S1 a) ESI mass spectrum of the [2]rotaxane **1**•4PF_6, b) zoom of the ESI mass spectrum of **1**•4PF_6 showing peaks associated with the $[M - 2PF_6]^{2+}$ ion at m/z = 1265.8072 and c) zoom of the ESI mass spectrum of **1**•4PF_6 showing peaks associated with the $[M - 3PF_6]^{3+}$ ion at m/z = 795.5521.

4 ESI mass spectrum of 2•4PF_6

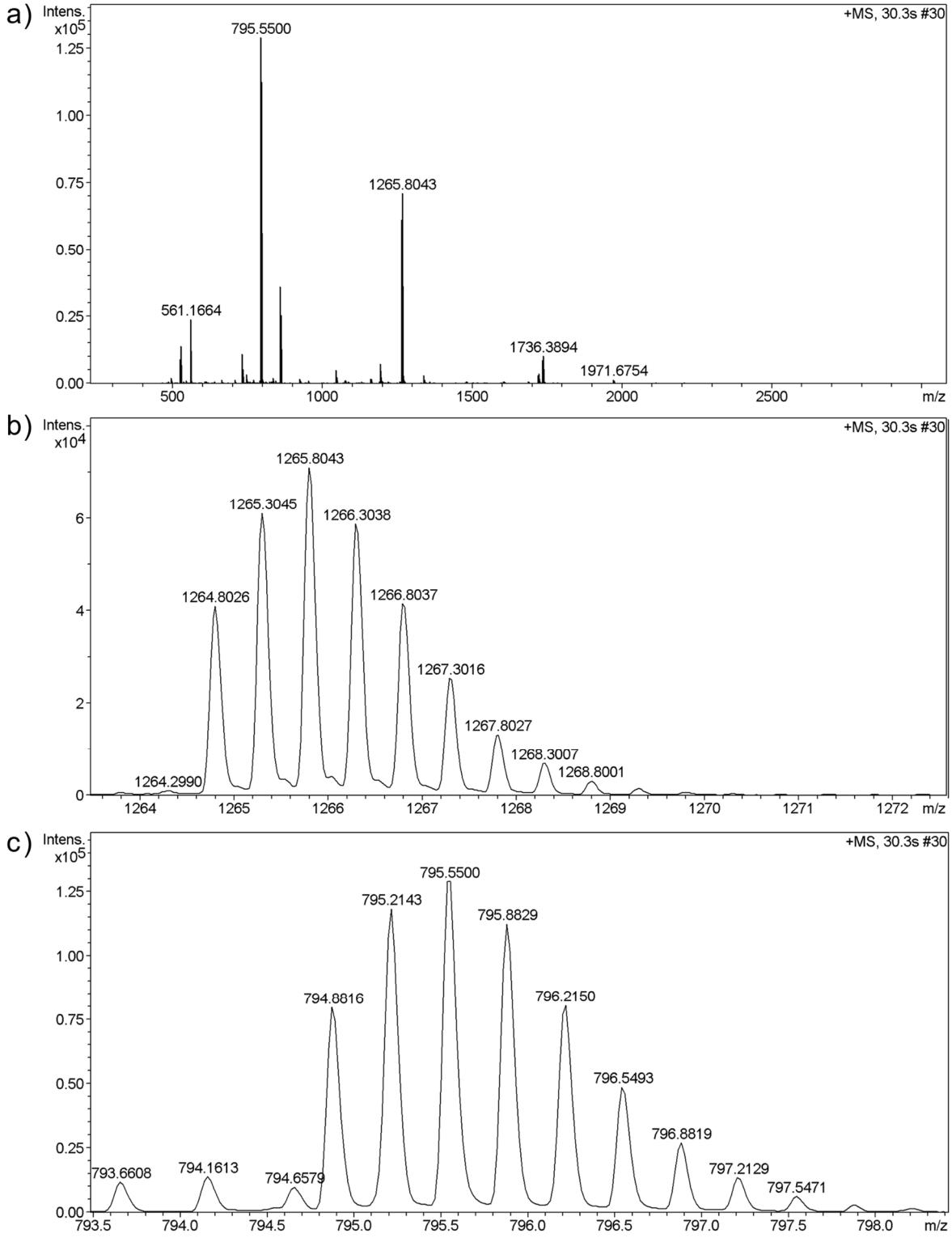

Fig. S2 a) ESI mass spectrum of the [2]rotaxane **2**•4PF_6, b) zoom of the ESI mass spectrum of **2**•4PF_6 showing peaks associated with the $[M - 2PF_6]^{2+}$ ion at m/z = 1265.8043 and c) zoom of the ESI mass spectrum of **2**•4PF_6 showing peaks associated with the $[M - 3PF_6]^{3+}$ ion at m/z = 795.5500.

5 UV/Vis/NIR absorption spectra of the dumbbells 14 and 24 and of the [2]rotaxanes 1^{4+} and 2^{4+}

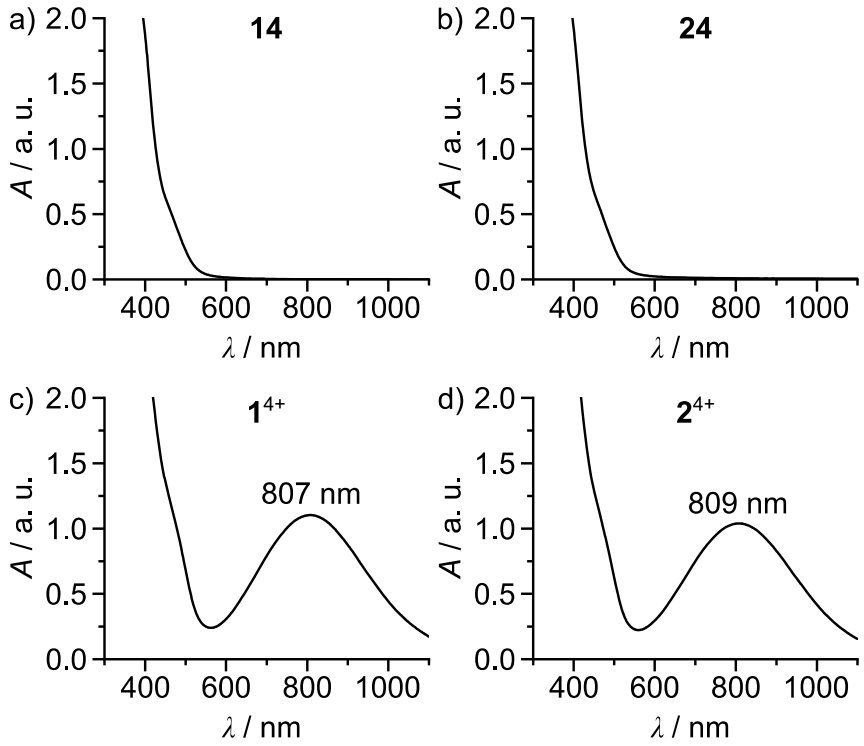

Fig. S3 UV/Vis/NIR absorption spectra recorded at 298 K of a) dumbbell **14** (0.4 mM, 1:1 MeCN/CH_2Cl_2), b) dumbbell **24** (0.4 mM, 1:1 MeCN/CH_2Cl_2), c) [2]rotaxane $\mathbf{1}^{4+}$ (0.6 mM, MeCN) and d) [2]rotaxane $\mathbf{2}^{4+}$ (0.6 mM, MeCN).

6 ^{1}H NMR spectrum of the dumbbell 14

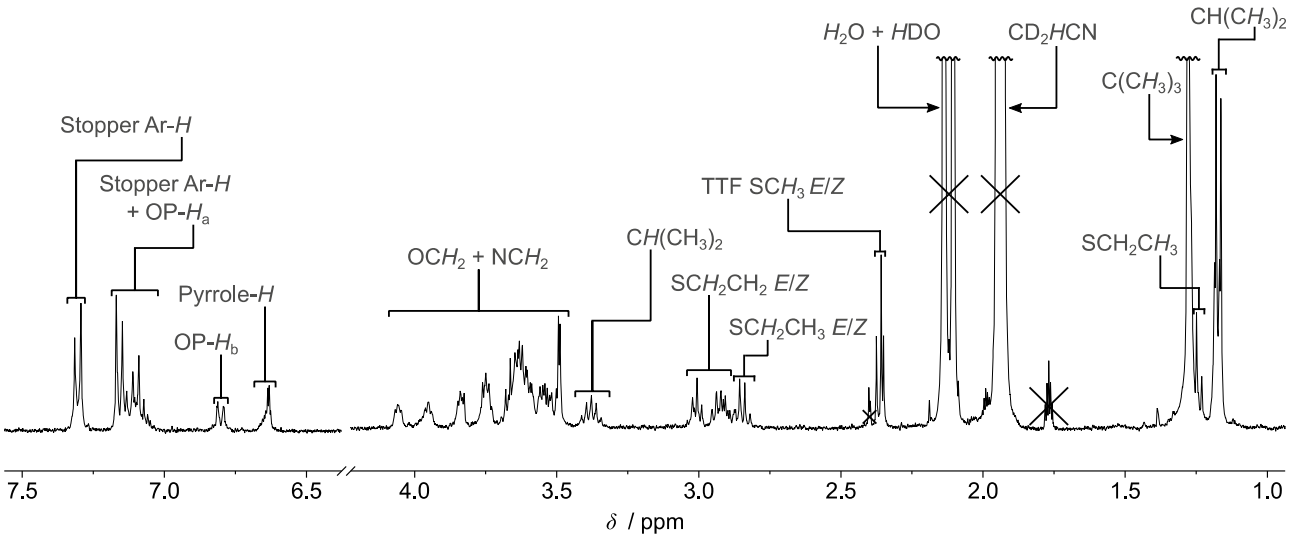

Fig. S4 Partial ^{1}H NMR spectrum of the dumbbell **14** (400 MHz, CD_3CN, 298 K, c < 1.5 mM). The $C(CH_3)_3$, CD_2HCN, HDO and H_2O signals are not shown in their full height.

7 COSY spectrum of 1•4PF$_6$

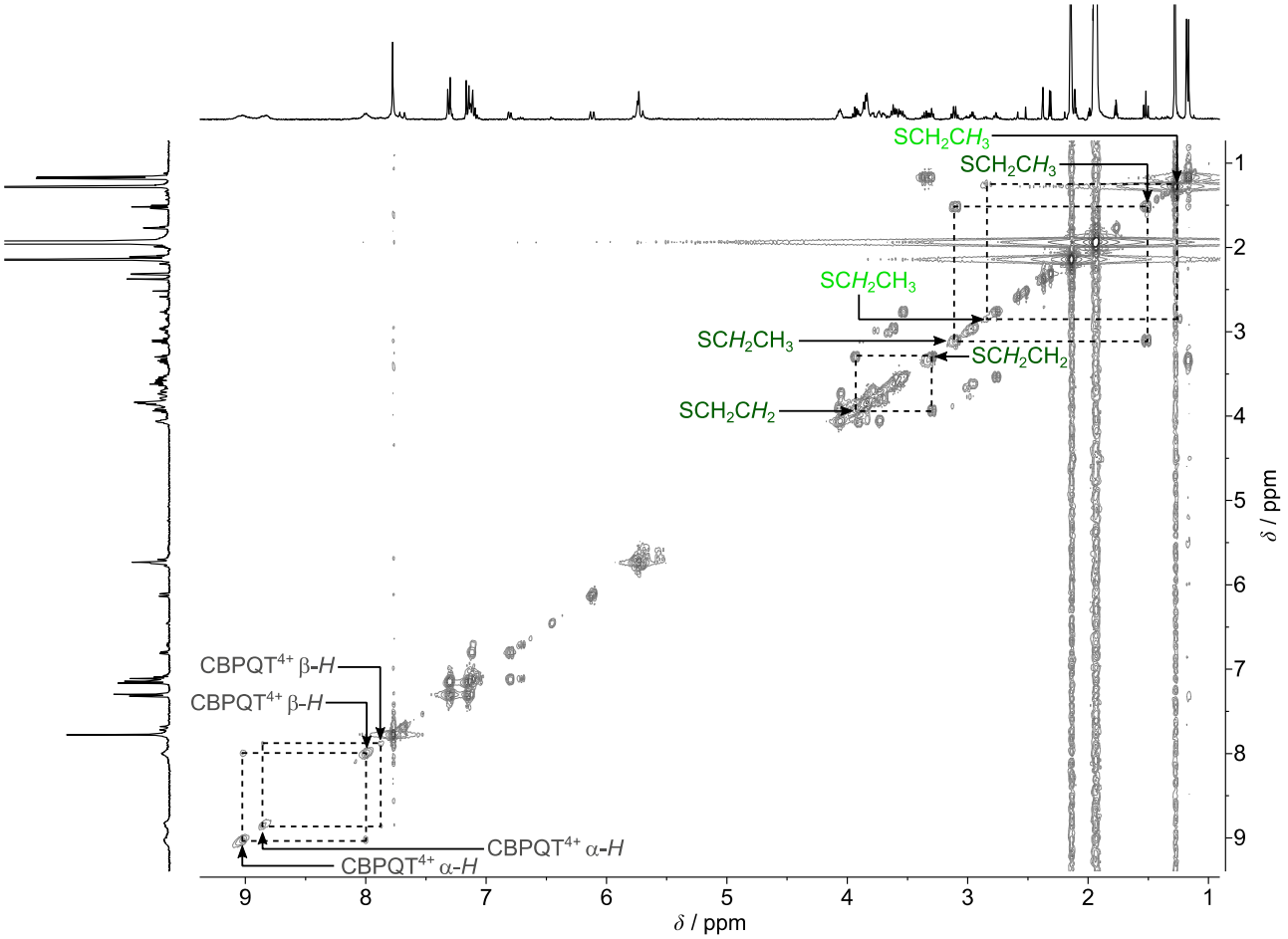

Fig. S5 Partial COSY spectrum of an isomeric mixture of the [2]rotaxane **1**$^{4+}$ (400 MHz, CD_3CN, 298 K, 1.5 mM), where the assignments in light green are associated with **1**•TTF^{4+} and the dark green signals are associated with **1**•MPTTF^{4+}, while the assignments in grey are associated with a mixture of the two translational isomers.

8 ^{1}H NMR spectrum of the dumbbell 24

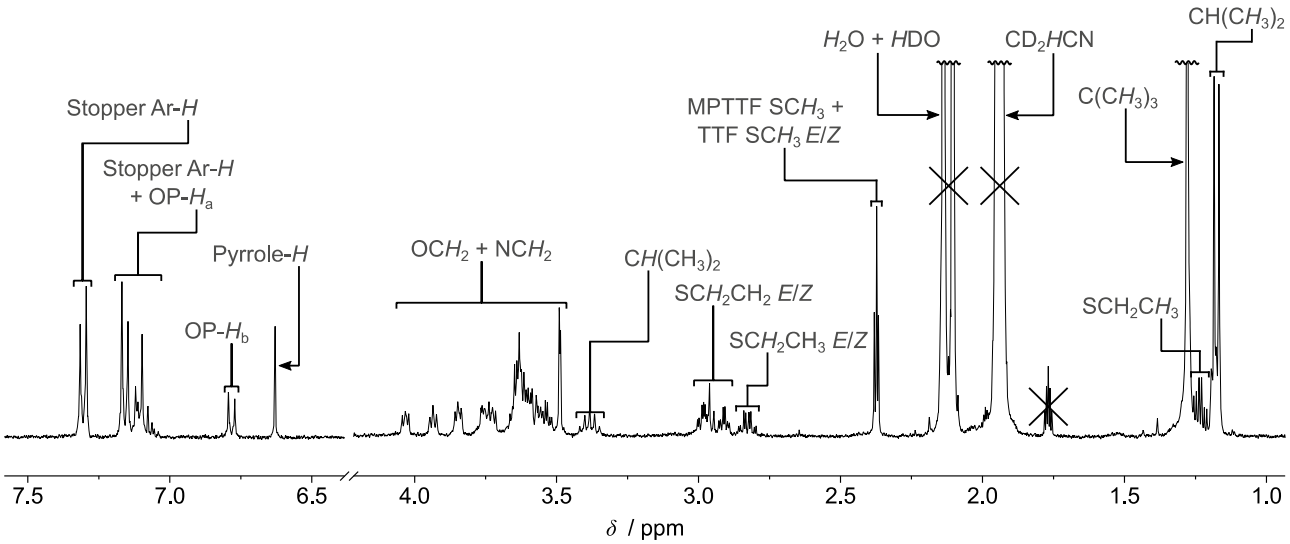

Fig. S6 Partial ^{1}H NMR spectrum of the dumbbell **24** (400 MHz, CD_3CN, 298 K, c < 1.5 mM). The $C(CH_3)_3$, CD_2HCN, HDO and H_2O signals are not shown in their full height.

9 ^{1}H NMR spectrum of 2•4PF$_6$

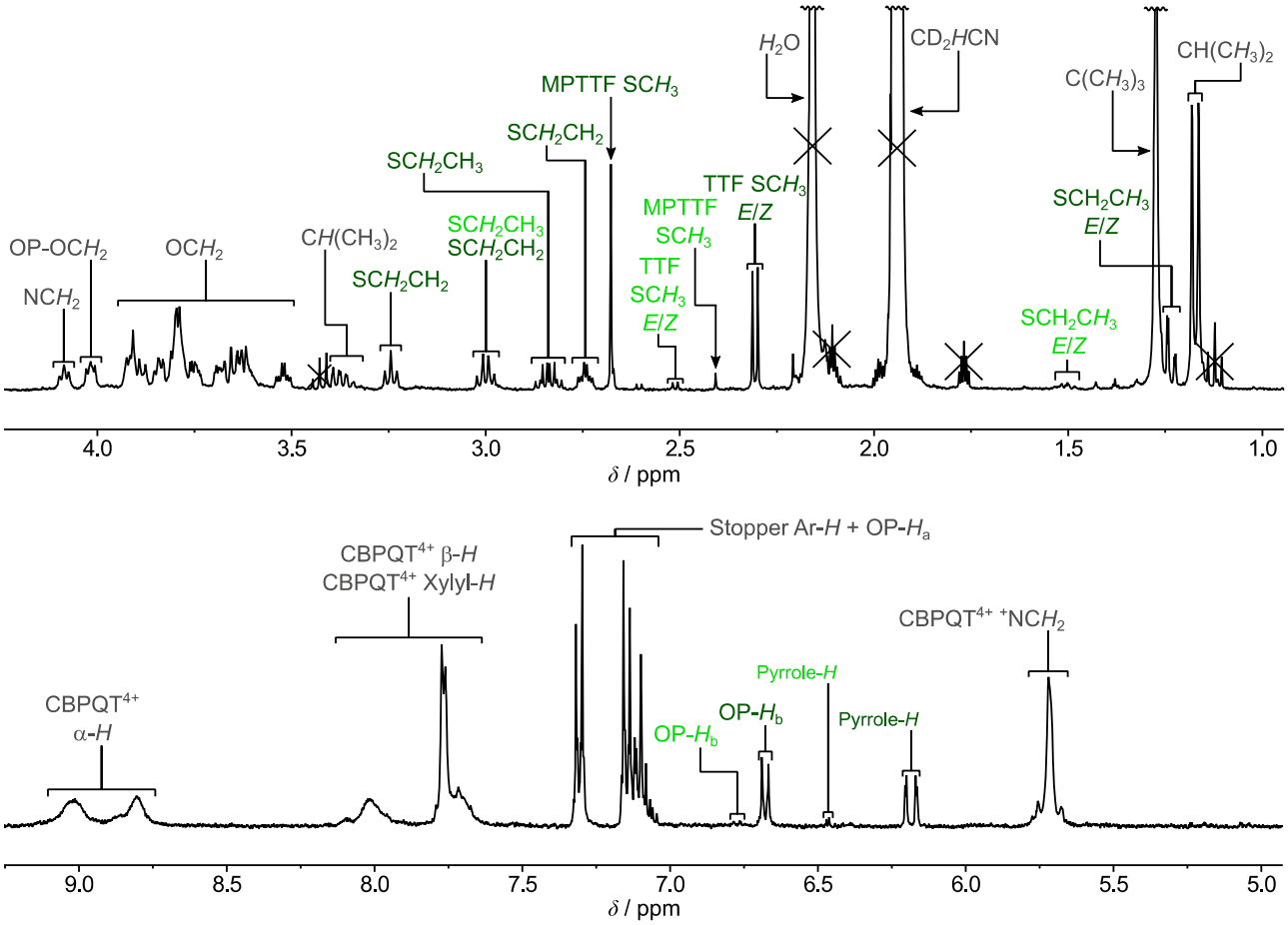

Fig. S7 Partial ^{1}H NMR spectrum of an isomeric mixture of the [2]rotaxane **2**$^{4+}$ (400 MHz, CD_3CN, 298 K, 1.5 mM), where the assignments in light green are associated with **2**•TTF^{4+} and the dark green signals are associated with **2**•MPTTF^{4+}, while the assignments in grey are associated with a mixture of the two translational isomers. The C(C*H*$_3$)$_3$, CD_2*H*CN and H_2O signals are not shown in their full height.

10 COSY spectrum of 2•4PF$_6$

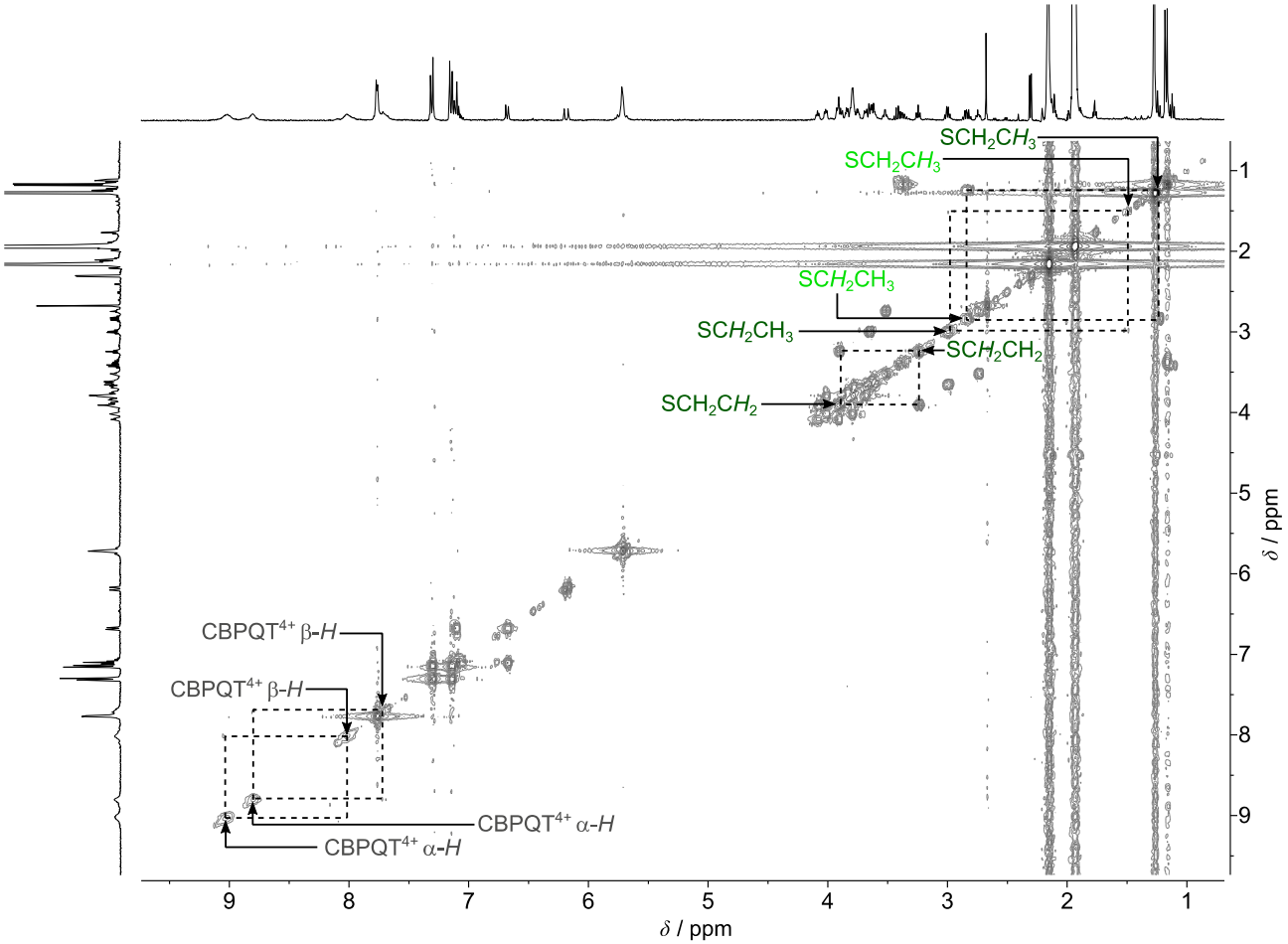

Fig. S8 Partial COSY spectrum of an isomeric mixture of the [2]rotaxane **2**$^{4+}$ (400 MHz, CD_3CN, 298 K, 1.5 mM), where the assignments in light green are associated with **2**•TTF^{4+} and the dark green signals are associated with **2**•MPTTF^{4+}, while the assignments in grey are associated with a mixture of the two translational isomers.

11 Calculations of the distribution between the two translational isomers in 1^{4+} and 2^{4+}

The relative amounts of the two translational isomers present in $\mathbf{1}^{4+}$ (*i.e.* **1**•MPTTF^{4+} and **1**•TTF^{4+}) and $\mathbf{2}^{4+}$ (*i.e.* **2**•MPTTF^{4+} and **2**•TTF^{4+}) were calculated using the integrals (*I*) from three different sets of signals in the ^{1}H NMR spectra recorded in CD_3CN at 298 K of $\mathbf{1}^{4+}$ (Fig. 2) and $\mathbf{2}^{4+}$ (Fig. S7), respectively, as probes. The distribution between the two translational isomers was calculated as an average of the three probes. Signals associated with the **1**•OP^{4+} and **2**•OP^{4+} translational isomers were not observed in the ^{1}H NMR spectra of $\mathbf{1}^{4+}$ and $\mathbf{2}^{4+}$.

Table S1 Distribution between the two translational isomers **1**•MPTTF^{4+} and **1**•TTF^{4+} determined by ^{1}H NMR spectroscopy in CD_3CN at 298 K using three different signals as probes

Signal	*δ* for **1**•MPTTF^{4+}/**1**•TTF^{4+} [ppm]	*I* of **1**•MPTTF^{4+}/**1**•TTF^{4+}	Relative amount of **1**•MPTTF^{4+}/**1**•TTF^{4+} [%]	Average relative amount of **1**•MPTTF^{4+}/**1**•TTF^{4+} [%]
TTF-SCH_3	2.31 + 2.32/2.52	2.14/0.50	81/19	82/18
TTF-SCH_3	2.37 + 2.38/2.58 + 2.59	2.21/0.51	81/19	
Pyrrole-*H*	6.11 + 6.14/6.44–6.48	1.41/0.27	84/16	

Table S2 Distribution between the two translational isomers **2**•MPTTF^{4+} and **2**•TTF^{4+} determined by ^{1}H NMR spectroscopy in CD_3CN at 298 K using three different signals as probes

Signal	*δ* for **2**•MPTTF^{4+}/**2**•TTF^{4+} [ppm]	*I* of **2**•MPTTF^{4+}/**2**•TTF^{4+}	Relative amount of **2**•MPTTF^{4+}/**2**•TTF^{4+} [%]	Average relative amount of **2**•MPTTF^{4+}/**2**•TTF^{4+} [%]
TTF-SCH_3	2.30 + 2.31/2.51 + 2.52	2.50/0.14	95/5	95/5
MPTTF-SCH_3	2.68/2.41	2.53/0.16	94/6	
Pyrrole-*H*	6.17 + 6.20/6.46 + 6.47	1.52/0.07	96/4	

12 Theoretical calculations of the ratio between the three translational isomers in 1^{4+} and 2^{4+}

The theoretical distribution of $CBPQT^{4+}$ encircling the three different stations (*i.e.* TTF, MPTTF and OP) at equilibrium was calculated using the relationship $K_{eq} = \exp[(\Delta\Delta G°)/RT]$ where $\Delta\Delta G°$ is the difference between the free energy of binding of the two stations in question, R is the gas constant and T is the absolute temperature. Since the rotaxane $\mathbf{1}^{4+}$ contains three stations, two ratios, each representing an equilibrium between two adjacent stations, needs to be combined. Since the MPTTF and OP stations both are adjacent to the TTF station, the two ratios in question are between $\mathbf{1}$•TTF^{4+} and $\mathbf{1}$•$MPTTF^{4+}$ and between $\mathbf{1}$•OP^{4+} and $\mathbf{1}$•TTF^{4+}, respectively. Using the free energies $\Delta G°(MPTTF)^{S10} = -6.0$ kcal mol^{-1}, $\Delta G°(TTF)^{S5} = -4.4$ kcal mol^{-1} and $\Delta G°(OP)^{S5} = -1.7$ kcal mol^{-1} in MeCN at 298 K, the ratios can be determined. Initially, the ratio representing the equilibrium between $\mathbf{1}$•TTF^{4+} and $\mathbf{1}$•$MPTTF^{4+}$ can be calculated:

$$\frac{K_{TTF}}{K_{MPTTF}} = e^{\left(\frac{((-6.0)-(-4.4))\text{kcal mol}^{-1}}{1.987\cdot10^{-3}\text{kcal K}^{-1}\text{ mol}^{-1}\cdot298\text{ K}}\right)} = 0.067$$

The ratio is converted into percentage of $\mathbf{1}$•TTF^{4+} relative to $\mathbf{1}$•$MPTTF^{4+}$:

$$\frac{0.067}{0.067 + 1} = 0.063 \approx 6\%$$

Thus, the ratio between $\mathbf{1}$•TTF^{4+} and $\mathbf{1}$•$MPTTF^{4+}$, respectively, is 6:94. The relationship representing the equilibrium between $\mathbf{1}$•OP^{4+} and $\mathbf{1}$•TTF^{4+} is calculated:

$$\frac{K_{OP}}{K_{TTF}} = e^{\left(\frac{((-4.4)-(-1.7))\text{kcal mol}^{-1}}{1.987\cdot10^{-3}\text{ kcal K}^{-1}\text{ mol}^{-1}\cdot298\text{ K}}\right)} = 0.010$$

$$\Rightarrow\frac{0.010}{0.010 + 1} = 0.010 \approx 1\%$$

Thus, the ratio between $\mathbf{1}$•OP^{4+} and $\mathbf{1}$•TTF^{4+}, respectively, is 1:99. If the percentages of $\mathbf{1}$•$MPTTF^{4+}$, $\mathbf{1}$•TTF^{4+} and $\mathbf{1}$•OP^{4+} are defined as x, y and z, respectively, the following relationships are obtained:

$$\text{A: } 94y = 6x$$
$$\text{B: } y = 99z$$
$$\text{C: } x + y + z = 100$$

By combining equations A and B, x can be determined in terms of z:

$$94\cdot99z = 6x \Leftrightarrow x = 1551z$$

To determine z, the expressions for x and y are inserted into equation C:

$$1551z + 99z + z = 100 \Leftrightarrow z = 0.06 \approx 0$$

By inserting z into the expressions for x and y, the latter two can be determined:

$$y = 99\cdot0.06 = 5.99 \approx 6$$
$$x = 1551\cdot0.06 = 93.94 \approx 94$$

To conclude, the calculated ratio between $\mathbf{1}$•$MPTTF^{4+}$, $\mathbf{1}$•TTF^{4+} and $\mathbf{1}$•OP^{4+}, respectively, is 94:6:0.

13 Suggested mechanism for oxidation of 14, 24 and 2•MPTTF^{4+}

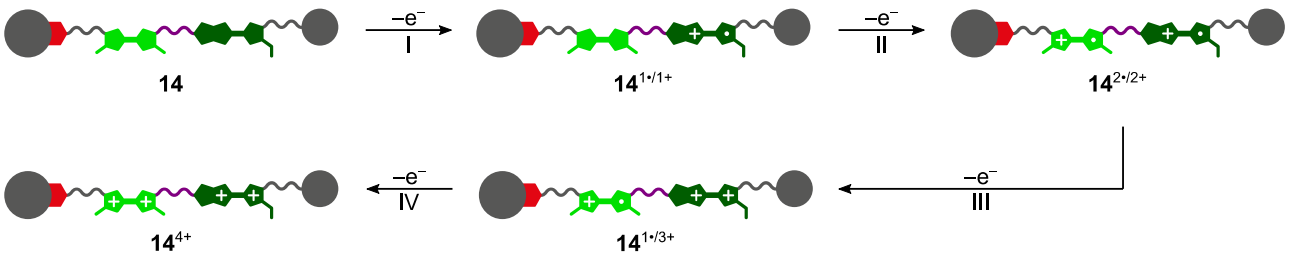

Scheme S4 Suggested mechanism for tetra-oxidation of the dumbbell **14** to produce **14**$^{4+}$.

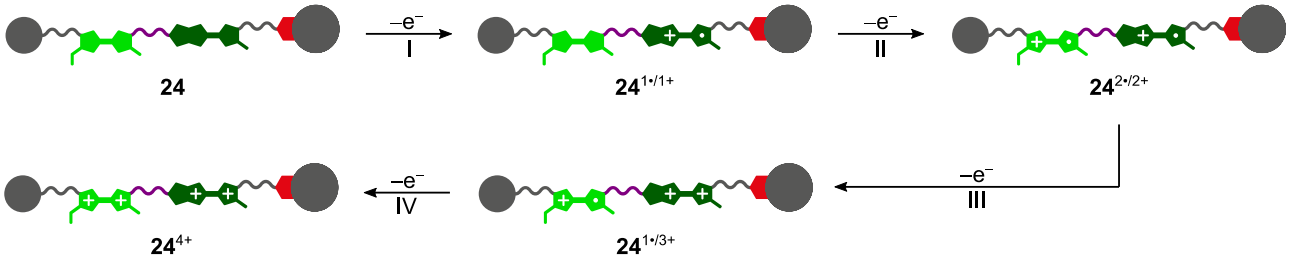

Scheme S5 Suggested mechanism for tetra-oxidation of the dumbbell **24** to produce **24**$^{4+}$.

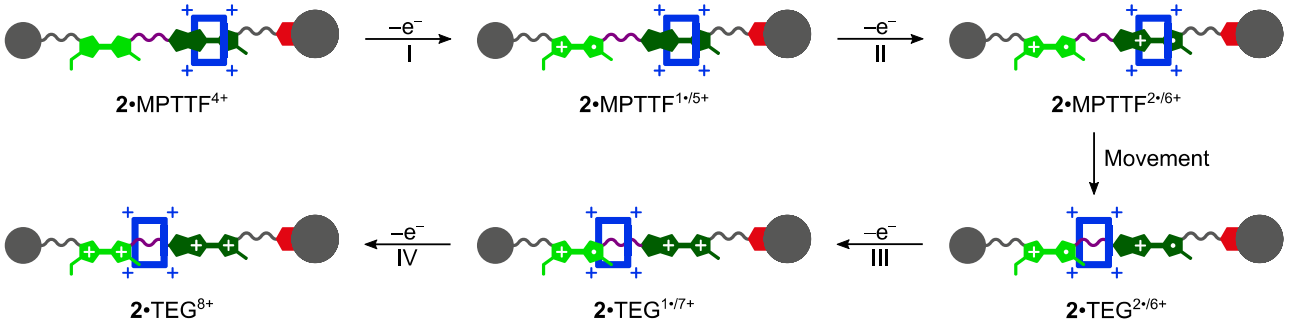

Scheme S6 Suggested mechanism for tetra-oxidation of **2**•MPTTF^{4+} to produce **2**•TEG^{8+} in which the CBPQT^{4+} ring is located on the TEG linker connecting the TTF^{2+} and MPTTF^{2+} dications.

14 ^{1}H NMR spectra of 1^{8+} recorded at 298 K 5 min and 18 min after oxidation

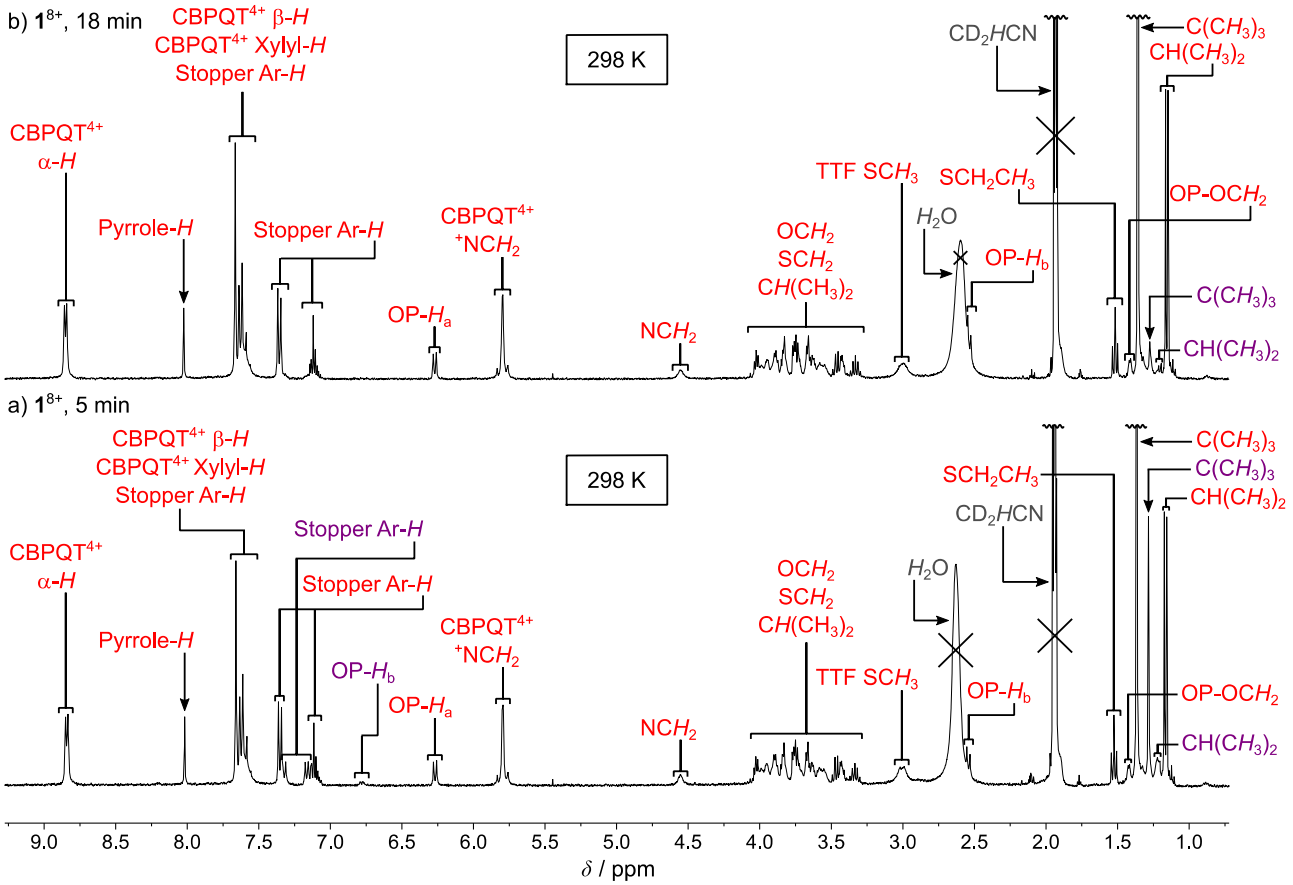

Fig. S9 Partial ^{1}H NMR spectra (400 MHz, CD_3CN, 298 K, 1.5 mM) recorded of a) the oxidised [2]rotaxane $\mathbf{1}^{8+}$, 5 min after mixing $\mathbf{1}^{4+}$ with 10 equiv. of tris(4-bromophenyl)ammoniumyl hexachloroantimonate ($TBPASbCl_6$) to produce $\mathbf{1}^{8+}$ and b) the oxidised [2]rotaxane $\mathbf{1}^{8+}$, 18 min after mixing $\mathbf{1}^{4+}$ with 10 equiv. of tris(4-bromophenyl)ammoniumyl hexachloroantimonate ($TBPASbCl_6$) to produce $\mathbf{1}^{8+}$. The assignments in red are associated with **1**•OP^{8+} (*i.e.* the OP station is located inside the $CBPQT^{4+}$ ring) and the assignments in purple are associated with **1**•TEG^{8+} (*i.e.* the $CBPQT^{4+}$ ring is located at the TEG linker connecting the TTF^{2+} and $MPTTF^{2+}$ dications). The $C(CH_3)_3$ and CD_2HCN signals are not shown in their full height.

15 COSY spectrum of 1^{8+} recorded at 298 K

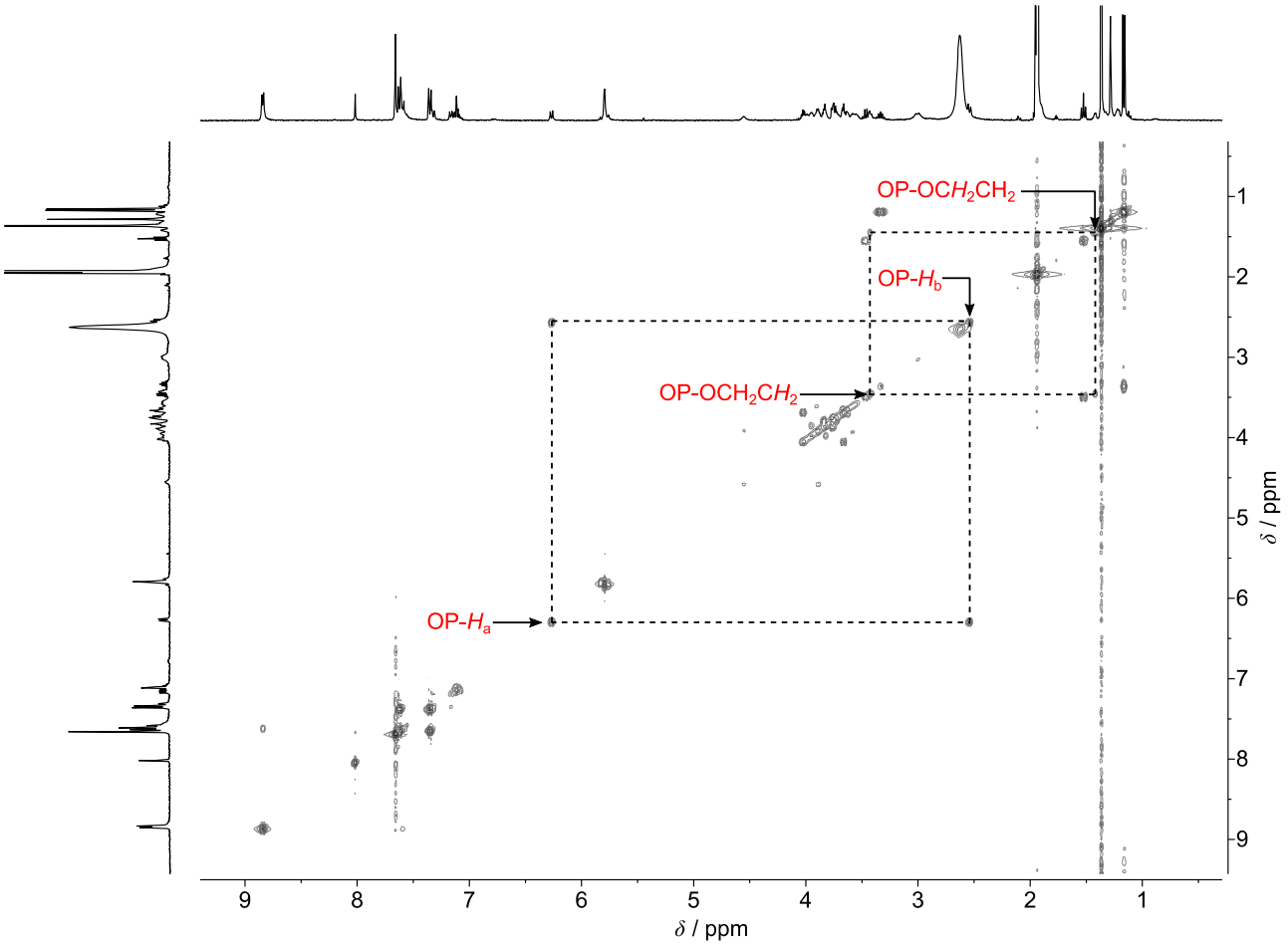

Fig. S10 Partial COSY spectrum of the oxidised [2]rotaxane $\mathbf{1}^{8+}$ (400 MHz, CD_3CN, 298 K, 1.5 mM), where the assignments in red are associated with **1**•OP^{8+}.

16 ^{1}H NMR spectra of 2^{8+} recorded at 298 K 5 min and 18 min after oxidation

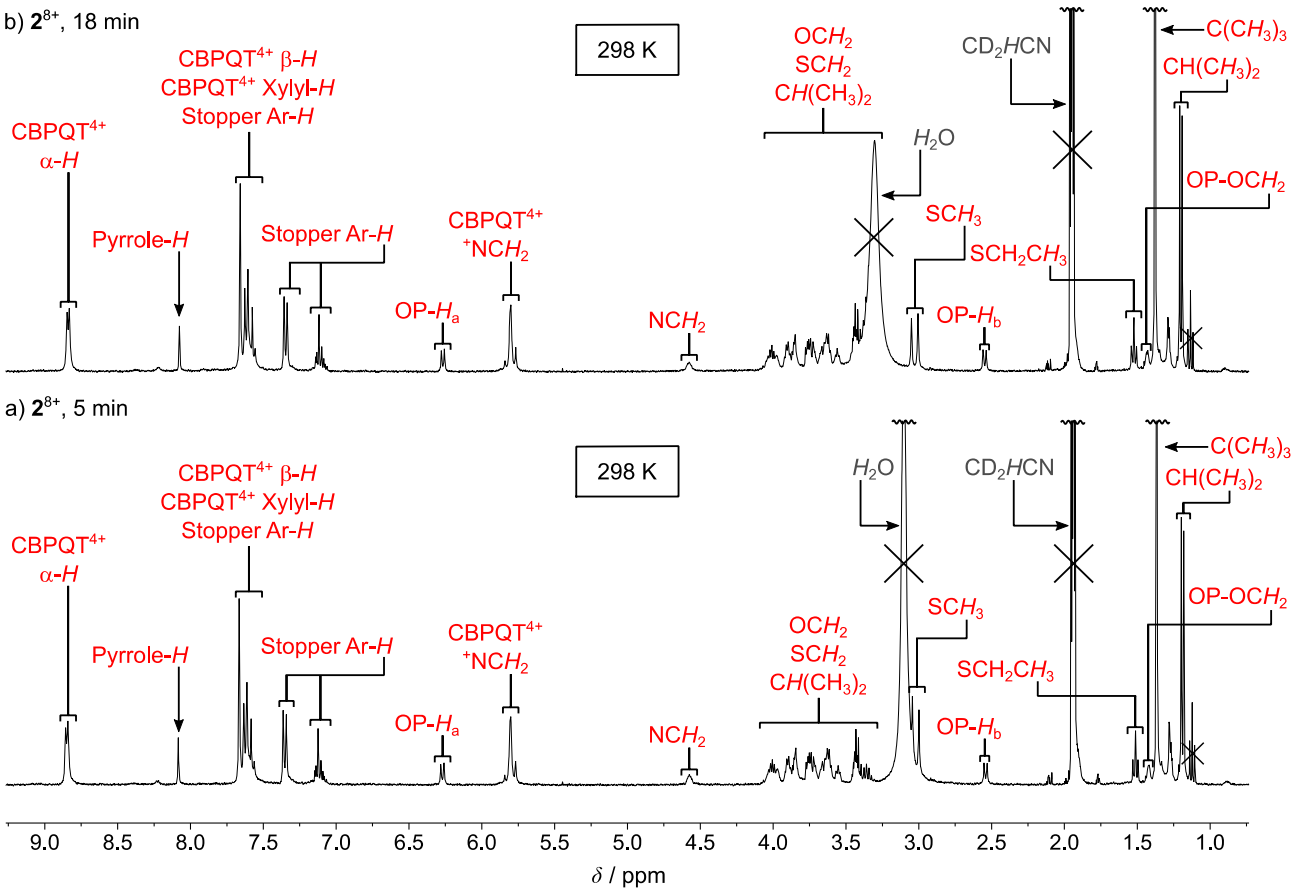

Fig. S11 Partial ^{1}H NMR spectra (400 MHz, CD_3CN, 298 K, 1.5 mM) recorded of a) the oxidised [2]rotaxane $\mathbf{2}^{8+}$, 5 min after mixing $\mathbf{2}^{4+}$ with 10 equiv. of tris(4-bromophenyl)ammoniumyl hexachloroantimonate ($TBPASbCl_6$) to produce $\mathbf{2}^{8+}$ and b) the oxidised [2]rotaxane $\mathbf{2}^{8+}$, 18 min after mixing $\mathbf{2}^{4+}$ with 10 equiv. of tris(4-bromophenyl)ammoniumyl hexachloroantimonate ($TBPASbCl_6$) to produce $\mathbf{2}^{8+}$. The assignments in red are associated with $\mathbf{2}$•OP^{8+} (*i.e.* the OP station is located inside the $CBPQT^{4+}$ ring). The $C(CH_3)_3$, H_2O and CD_2HCN signals are not shown in their full height.

17 COSY spectrum of 2^{8+} recorded at 298 K

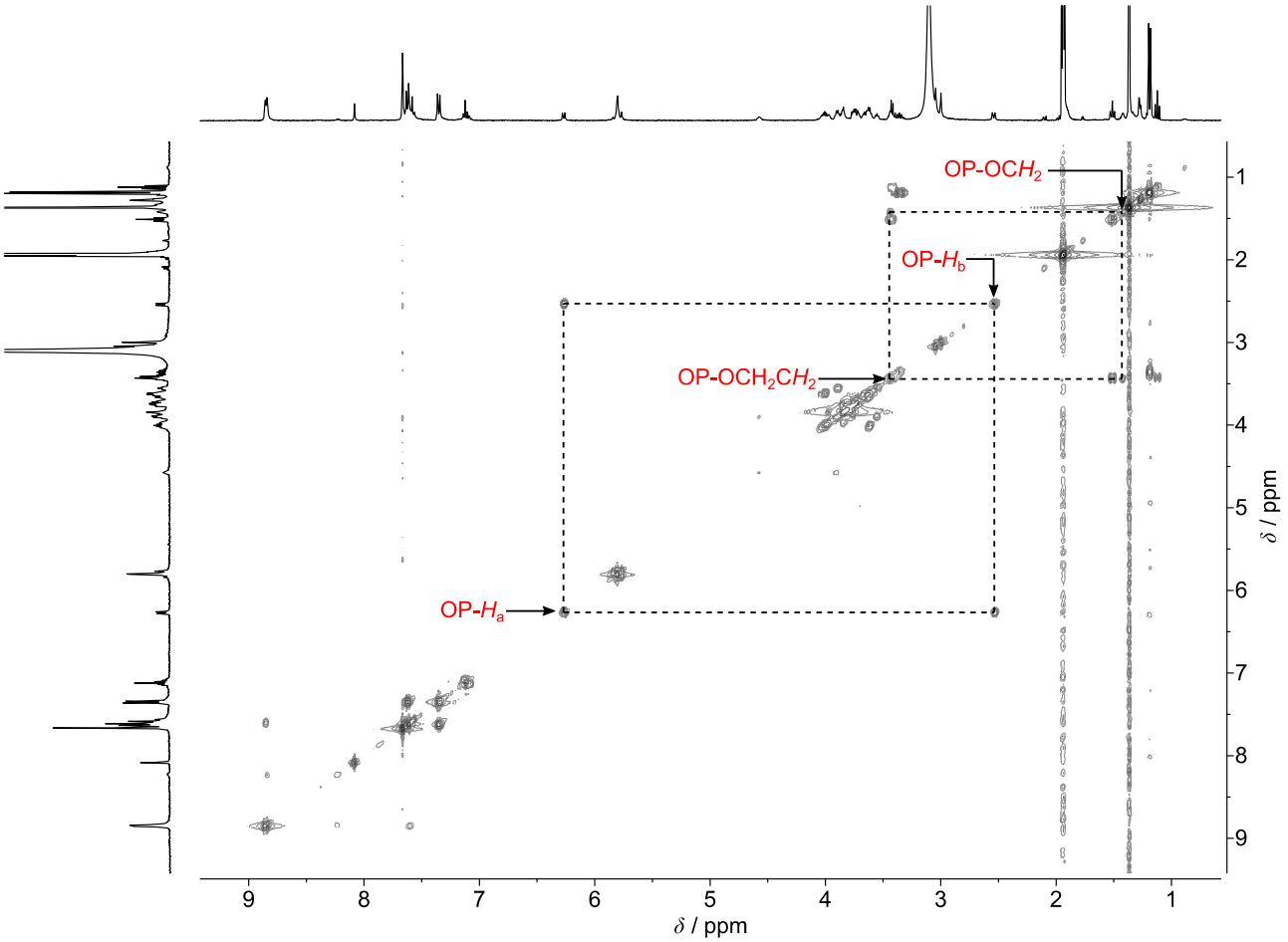

Fig. S12 Partial COSY spectrum of the oxidised [2]rotaxane $\mathbf{2}^{8+}$ (400 MHz, CD_3CN, 298 K, 1.5 mM), where the assignments in red are associated with $\mathbf{2}$•OP^{8+}.

18 ^{1}H NMR spectra of 2^{8+} recorded at 298 K and 253 K

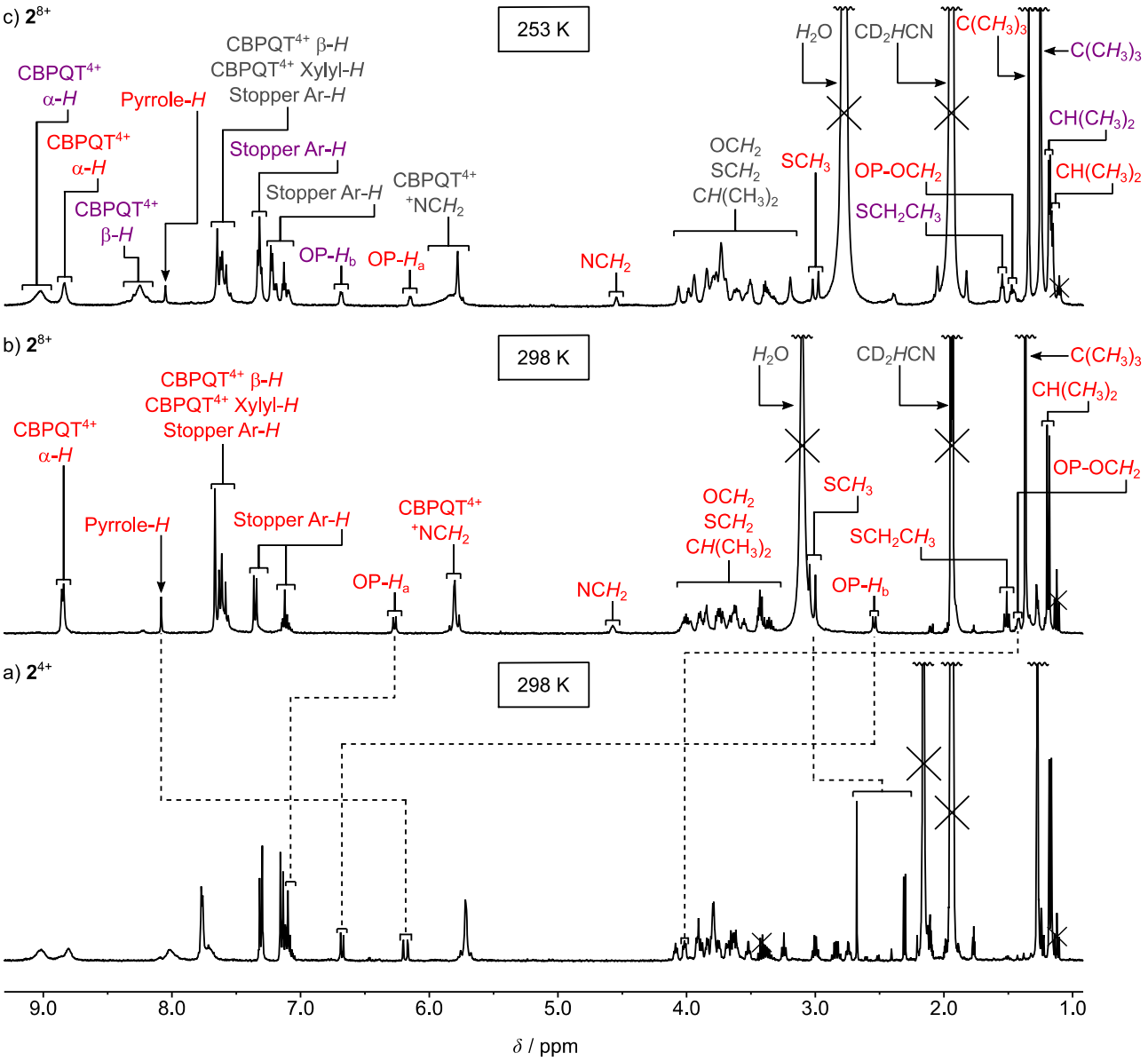

Fig. S13 Partial ^{1}H NMR spectra (CD_3CN, 1.5 mM) recorded of a) the [2]rotaxane $\mathbf{2}^{4+}$ (400 MHz) at 298 K, b) the oxidised [2]rotaxane $\mathbf{2}^{8+}$ (400 MHz) at 298 K and c) the oxidised [2]rotaxane $\mathbf{2}^{8+}$ (600 MHz) at 253 K. $\mathbf{2}^{8+}$ was generated by adding an excess of the chemical oxidant tris(4-bromophenyl)ammoniumyl hexachloroantimonate ($TBPASbCl_6$) to $\mathbf{2}^{4+}$ and the spectra were recorded *ca.* 5 min after adding $TBPASbCl_6$ at the indicated temperature. The assignments in red are associated with $\mathbf{2}$•OP^{8+} (*i.e.* the OP station is located inside the $CBPQT^{4+}$ ring) and the assignments in purple are associated with $\mathbf{2}$•TEG^{8+} (*i.e.* the $CBPQT^{4+}$ ring is located at the TEG linker connecting the TTF^{2+} and $MPTTF^{2+}$ units). The $C(CH_3)_3$, H_2O and CD_2HCN signals are not shown in their full height.

19 ^{1}H NMR spectrum of the oxidised dumbbell 14^{4+}

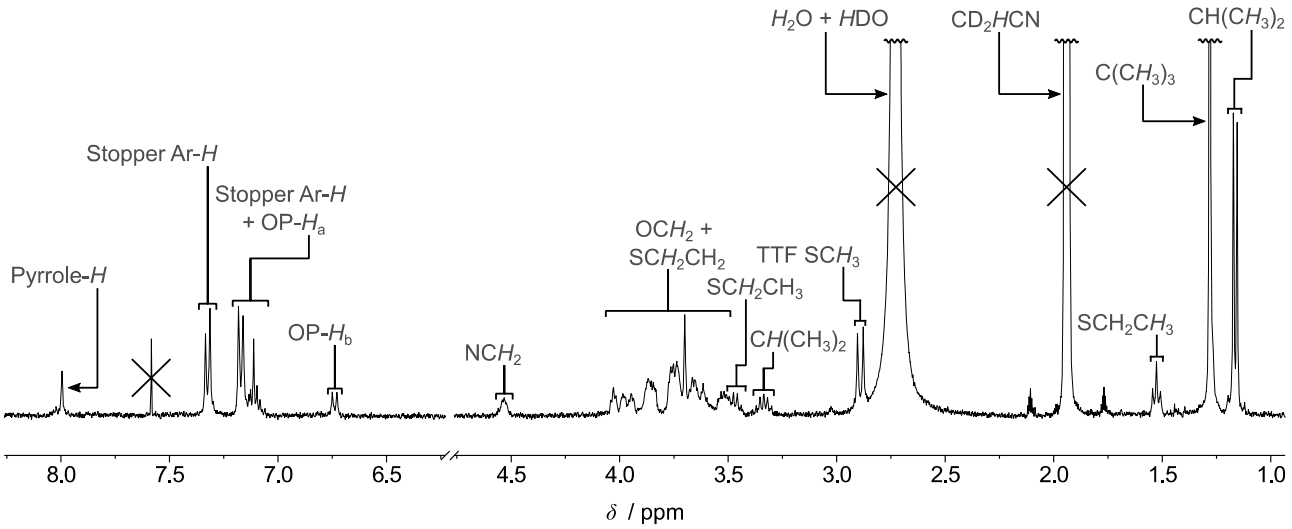

Fig. S14 Partial ^{1}H NMR spectrum of the oxidised dumbbell $\mathbf{14}^{4+}$ (400 MHz, CD_3CN, 298 K, c < 1.5 mM), where **14** was mixed with 10 equiv. of $TBPASbCl_6$ to produce $\mathbf{14}^{4+}$. The $C(CH_3)_3$, CD_2HCN, H_2O and HDO signals are not shown in their full height.

20 ^{1}H NMR spectrum of the oxidised dumbbell 24^{4+}

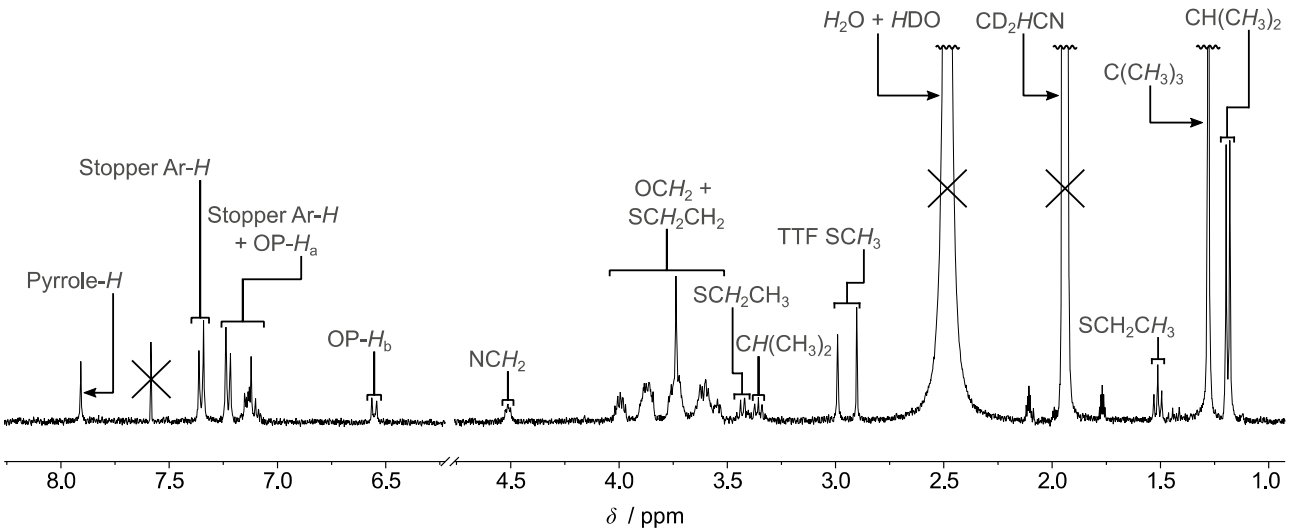

Fig. S15 Partial ^{1}H NMR spectrum of the oxidised dumbbell $\mathbf{24}^{4+}$ (400 MHz, CD_3CN, 298 K, c < 1.5 mM), where **24** was mixed with 10 equiv. of $TBPASbCl_6$ to produce $\mathbf{24}^{4+}$. The $C(CH_3)_3$, CD_2HCN, H_2O and HDO signals are not shown in their full height.

21 A series of ^{1}H NMR spectra of 1^{8+} recorded at 258 K

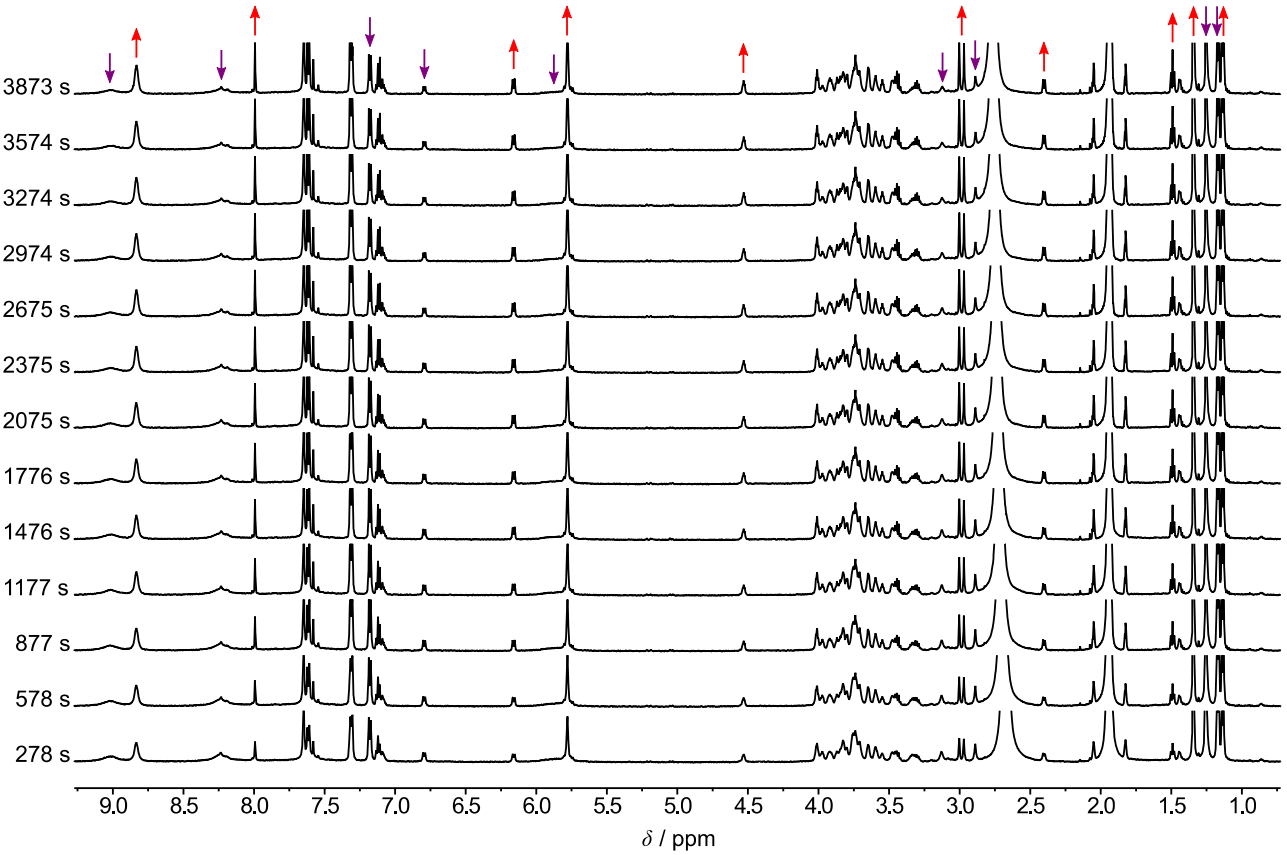

Fig. S16 The first 13 ^{1}H NMR spectra (600 MHz, CD_3CN, 258 K, 1.5 mM) recorded of $\mathbf{1}^{8+}$ showing the change in signals in the first 3873 s after oxidising $\mathbf{1}^{4+}$ to $\mathbf{1}^{8+}$ with an excess of $TBPASbCl_6$. Red arrows indicate increasing signals for **1**•OP^{8+}, while purple arrows indicate decreasing signals for **1**•TEG^{8+}. Not all signals are shown in their full height.

22 A series of ^{1}H NMR spectra of 2^{8+} recorded at 253 K

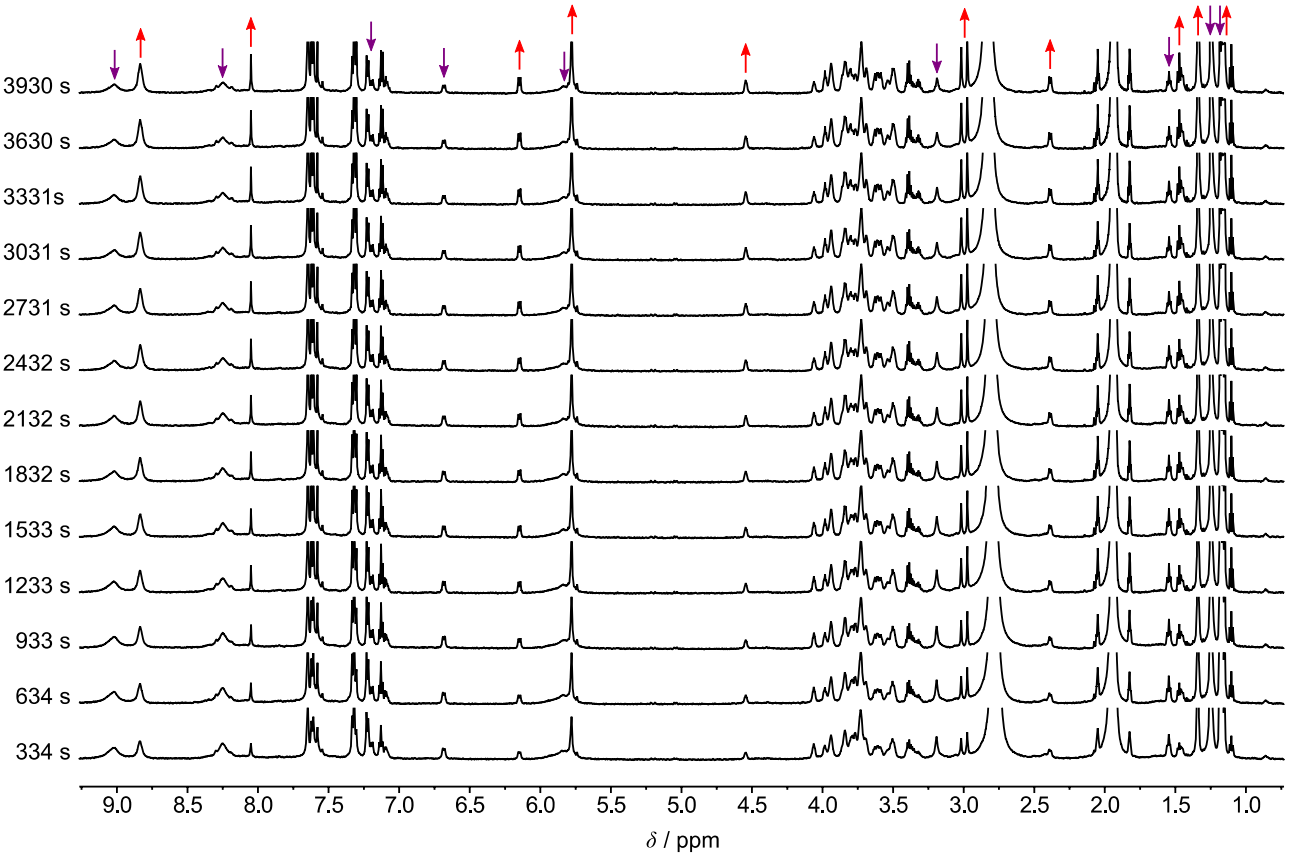

Fig. S17 The first 13 ^{1}H NMR spectra (600 MHz, CD_3CN, 253 K, 1.5 mM) recorded of $\mathbf{2}^{8+}$ showing the change in signals in the first 3930 s after oxidising $\mathbf{2}^{4+}$ to $\mathbf{2}^{8+}$ with an excess of $TBPASbCl_6$. Red arrows indicate increasing signals for $\mathbf{2}$•OP^{8+}, while purple arrows indicate decreasing signals for $\mathbf{2}$•TEG^{8+}. Not all signals are shown in their full height.

23 ^{1}H NMR spectra of 2^{8+} recorded at 253 K at different delay times after oxidation

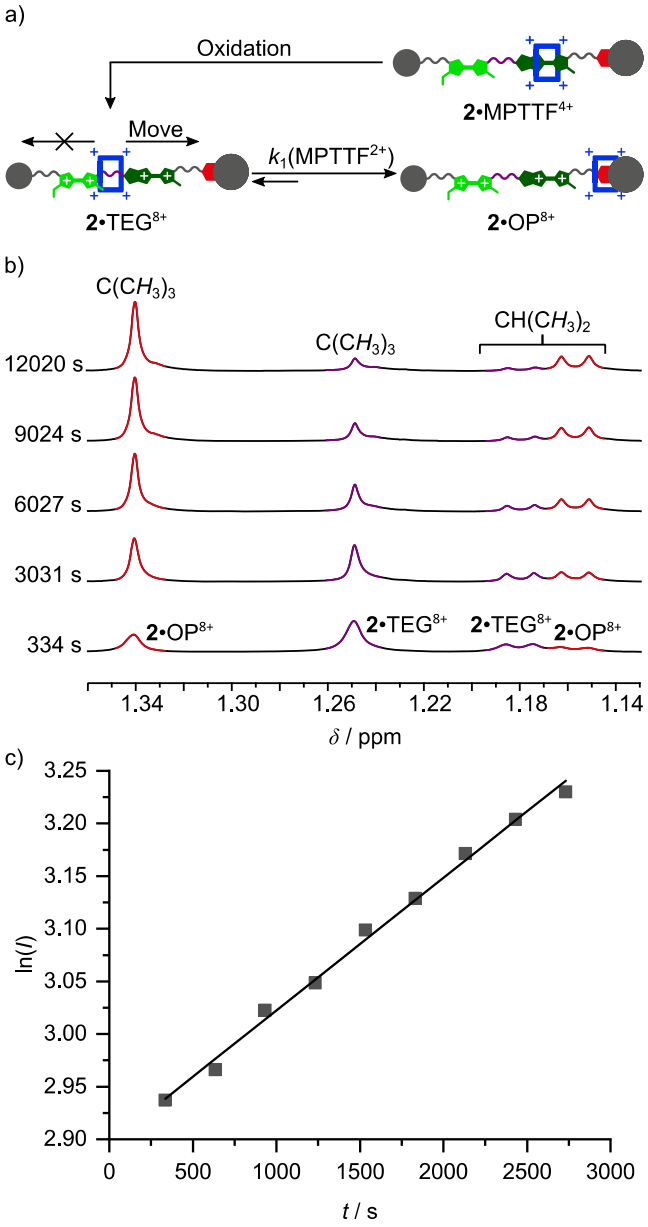

Fig. S18 a) A cartoon representation illustrating the oxidation of **2**•MPTTF^{4+} leading initially to the formation of **2**•TEG^{8+} followed by the movement of CBPQT^{4+} across the MPTTF dication (*i.e.* MPTTF^{2+}) to produce **2**•OP^{8+}. b) A series of partial ^{1}H NMR spectra (600 MHz, 253 K, CD_3CN) of the oxidised [2]rotaxane $\mathbf{2}^{8+}$ recorded at different delay times after addition of an excess (28–32 equiv.) of $TBPASbCl_6$ to $\mathbf{2}^{4+}$ (c = 1.5 mM) showing the increasing signals for the resonances associated with the $C(CH_3)_3$ protons (δ = 1.34 ppm) and the $CH(CH_3)_2$ protons (δ = 1.16 ppm), respectively, in **2**•OP^{8+}, and the decreasing signals for the resonances associated with the $C(CH_3)_3$ protons (δ = 1.25 ppm) and the $CH(CH_3)_2$ protons (δ = 1.18 ppm), respectively, in **2**•TEG^{8+}. c) Plot of ln I against t at 253 K for the movement of CBPQT^{4+} across the MPTTF^{2+} unit, where I is the integral of

the signal at δ = 1.34 ppm. The eight data points have been fitted by the best straight line (black line), giving a correlation coefficient of 0.995, indicating that first-order kinetics are in operation. The slope of the line corresponds to the rate constant k_1 for the movement of $CBPQT^{4+}$ over the $MPTTF^{2+}$ unit in $\mathbf{2}^{8+}$, according to the relationship $\ln I = k_1 t$.

24 First-order analysis

This section provides further information about the kinetic investigations carried out on $\mathbf{1}^{8+}$ and $\mathbf{2}^{8+}$ at different temperatures.

Initially, a baseline and phase correction were performed on all ^{1}H NMR spectra, whereupon the TMS signal was integrated and normalised to 100 and then used as an internal reference. All signals that did not overlap with any other signal were used as probes. At each temperature and for each probe, first-order kinetics were observed to be in operation, *i.e.* straight lines are observed when ln *I* is plotted against *t*, where *I* is the integral of the signal in question and *t* is the time. This outcome is a consequence of the fact that the data points (*n*) were collected in the early stage of the experiments where the reverse process is not yet occurring to any significant extent. The slope of the line corresponds to the rate constant k_1 for the movement of $CBPQT^{4+}$ over the TTF^{2+} unit in $\mathbf{1}^{8+}$ or over the $MPTTF^{2+}$ unit in $\mathbf{2}^{8+}$ according to the relationship $\ln I = k_1 t$. Only probes that upon linear regression gave a straight line with $R^2 > 0.9$ were used. The k_1 values and the corresponding free energies of activation[S11] ($\Delta G^{\ddagger}(k_1)$) obtained from these experiments are recorded in Tables S3 and S4. Finally, the rate constant (k_1^{av}) and the derived energy of activation $\Delta G^{\ddagger}(k_1^{av})$ for the movement of $CBPQT^{4+}$ from the TEG linker to the OP unit at each temperature were obtained (Table 2) as an average of the k_1 values obtained for each of the different probes collected in Tables S3 and S4.

Table S3 Rate constants (k_1) and derived free energies of activations ($\Delta G^{\ddagger}(k_1)$) for the movement of $CBPQT^{4+}$ over the TTF^{2+} unit in $\mathbf{1}^{8+}$ for probes having correlation coefficients $R^2 > 0.9$ at 243, 253, 258, 263 and 268 K, together with the number of data points (n) included in the linear regression. The purple probes are associated with $\mathbf{1}\bullet TEG^{8+}$ and the red probes are associated with $\mathbf{1}\bullet OP^{8+}$

T [K]	Probe	δ [ppm]	n	k_1 [10^{-4} s^{-1}][a]	$\Delta G^{\ddagger}(k_1)$ [kcal mol^{-1}][a]	R^2
243	$CBPQT^{4+}$ α-*H*	8.93–9.31	6	0.98 ± 0.11	18.60 ± 0.06	0.953
	Stopper Ar-*H*	7.20	6	0.36 ± 0.08	19.09 ± 0.11	0.948
	$C(CH_3)_3$	1.26	6	0.33 ± 0.02	19.12 ± 0.04	0.967
	$CH(CH_3)_2$	1.17	6	0.56 ± 0.06	18.87 ± 0.05	0.964
	$CBPQT^{4+}$α-*H*	8.85	6	0.70 ± 0.12	18.77 ± 0.08	0.904
	$C(CH_3)_3$	1.35	6	0.28 ± 0.05	19.21 ± 0.08	0.980
253	$CBPQT^{4+}$ α-*H*	8.90–9.29	8	0.94 ± 0.08	19.40 ± 0.05	0.917
	Stopper Ar-*H*	7.18	8	0.81 ± 0.07	19.48 ± 0.05	0.994
	OP-H_b	6.79	8	0.88 ± 0.31	19.44 ± 0.18	0.982
	$C(CH_3)_3$	1.25	8	0.78 ± 0.02	19.50 ± 0.03	0.997
	$CH(CH_3)_2$	1.17	8	0.80 ± 0.04	19.49 ± 0.03	0.996
	$CBPQT^{4+}$ α-*H*	8.83	8	0.74 ± 0.11	19.53 ± 0.08	0.989
	OP-H_a	6.15	8	0.97 ± 0.57	19.39 ± 0.30	0.966
	SCH_2CH_3	1.49	8	0.55 ± 0.22	19.68 ± 0.20	0.925
	$C(CH_3)_3$	1.34	8	0.84 ± 0.03	19.46 ± 0.03	1.000
	$CH(CH_3)_2$	1.13	8	0.84 ± 0.06	19.46 ± 0.04	0.968
258	$CBPQT^{4+}$ β-*H*	8.09–8.44	7	1.52 ± 0.08	19.55 ± 0.03	0.922
	Stopper Ar-*H*	7.18	7	1.30 ± 0.08	19.63 ± 0.04	0.994
	OP-H_b	6.79	7	2.27 ± 0.39	19.35 ± 0.09	0.926
	$C(CH_3)_3$	1.26	7	1.13 ± 0.02	19.71 ± 0.03	0.993
	$CH(CH_3)_2$	1.17	7	1.15 ± 0.05	19.70 ± 0.03	0.989
	$C(CH_3)_3$	1.34	7	0.87 ± 0.02	19.84 ± 0.03	0.998
	$CH(CH_3)_2$	1.13	7	0.89 ± 0.05	19.83 ± 0.04	0.977
263	$CBPQT^{4+}$ α-*H*	8.90–9.26	5	1.96 ± 0.14	19.81 ± 0.04	0.914
	Stopper Ar-*H*	7.18	5	1.70 ± 0.12	19.88 ± 0.04	0.997
	OP-H_b	6.80	5	1.31 ± 0.50	20.02 ± 0.20	0.973
	$C(CH_3)_3$	1.26	5	1.73 ± 0.03	19.87 ± 0.03	0.999
	$CH(CH_3)_2$	1.18	5	1.71 ± 0.07	19.88 ± 0.03	0.999
	$CBPQT^{4+}$ α-*H*	8.84	5	2.08 ± 0.15	19.78 ± 0.04	0.999
	Pyrrole-*H*	8.00	5	1.78 ± 0.49	19.86 ± 0.15	0.990
	OP-H_a	6.18	5	2.36 ± 0.66	19.71 ± 0.15	0.931
	SCH_2CH_3	1.50	5	1.92 ± 0.35	19.82 ± 0.10	0.996
	OCH_2	1.41–1.46	5	1.58 ± 0.44	19.92 ± 0.15	0.977
	$C(CH_3)_3$	1.35	5	2.14 ± 0.05	19.76 ± 0.03	0.997
	$CH(CH_3)_2$	1.14	5	2.15 ± 0.10	19.76 ± 0.03	0.996
268	Stopper Ar-*H*	7.18	5	2.79 ± 0.12	20.01 ± 0.03	1.000
	OP-H_b	6.80	5	1.31 ± 0.50	20.02 ± 0.20	0.973
	$C(CH_3)_3$	1.26	5	2.56 ± 0.03	20.05 ± 0.02	0.999
	$CH(CH_3)_2$	1.18	5	2.66 ± 0.07	20.03 ± 0.03	1.000
	$CBPQT^{4+}$ α-*H*	8.76–8.89	5	2.43 ± 0.12	20.08 ± 0.03	0.996

Pyrrole-*H*	8.00	5	2.55 ± 0.58	20.06 ± 0.12	1.000
OP-H_a	6.19	5	2.67 ± 0.52	20.03 ± 0.11	0.983
NCH_2	4.54	5	3.58 ± 0.57	19.87 ± 0.09	0.984
OP-H_b	2.44	5	2.35 ± 0.53	20.10 ± 0.12	0.938
SCH_2CH_3	1.50	5	1.94 ± 0.28	20.20 ± 0.08	0.993
OCH_2	1.40–1.46	5	1.18 ± 0.34	20.47 ± 0.15	0.976
C$(CH_3)_3$	1.35	5	2.65 ± 0.04	20.04 ± 0.02	0.990
CH$(CH_3)_2$	1.14	5	2.54 ± 0.07	20.06 ± 0.03	0.998

[a]The errors are calculated using the method presented in Koumura *et al.*[S12] with ΔT = 0.3 K, I = 5% and t = 0.1 s.

Taking an average of the probes with $R^2 > 0.9$ at the five different temperatures, yielded a rate constant (k_1^{av}) for each temperature, which are listed in Table 2.

Table S4 Rate constants (k_1) and derived free energies of activations ($\Delta G^{\ddagger}(k_1)$) for the movement of $CBPQT^{4+}$ over the $MPTTF^{2+}$ unit in $\mathbf{2}^{8+}$ for probes having correlation coefficients $R^2 > 0.9$ at 243, 253, 263 and 268 K, together with the number of data points (n) included in the linear regression. The purple probes are associated with $\mathbf{2}$•TEG^{8+} and the red probes are associated with $\mathbf{2}$•OP^{8+}

T [K]	Probe	δ [ppm]	n	k_1 [10^{-4} s^{-1}][a]	$\Delta G^{\ddagger}(k_1)$ [kcal mol^{-1}][a]	R^2
243	Stopper Ar-*H*	7.24	19	0.39 ± 0.04	19.05 ± 0.05	0.982
	SCH_2CH_3	1.54	19	0.38 ± 0.05	19.06 ± 0.07	0.903
	$C(CH_3)_3$	1.24	19	0.35 ± 0.01	19.10 ± 0.03	0.971
	$CH(CH_3)_2$	1.17	19	0.43 ± 0.02	19.00 ± 0.03	0.979
	Stopper Ar-*H*	7.30	19	0.29 ± 0.04	19.18 ± 0.07	0.939
	$C(CH_3)_3$	1.34	19	0.30 ± 0.01	19.18 ± 0.03	0.972
	$CH(CH_3)_2$	1.15	19	0.41 ± 0.02	19.02 ± 0.04	0.970
253	$CBPQT^{4+}$ α-*H*	8.92–9.27	9	1.53 ± 0.06	19.16 ± 0.03	0.925
	$CBPQT^{4+}$ β-*H*	8.12–8.44	9	1.21 ± 0.05	19.28 ± 0.03	0.965
	$C(CH_3)_3$	1.25	9	1.10 ± 0.01	19.33 ± 0.02	0.992
	$CH(CH_3)_2$	1.18	9	1.28 ± 0.04	19.25 ± 0.03	0.995
	$CBPQT^{4+}$ α-*H*	8.84	9	1.04 ± 0.07	19.36 ± 0.04	0.932
	CH_2N^+	5.78	9	0.93 ± 0.06	19.41 ± 0.04	0.922
	$C(CH_3)_3$	1.34	9	1.26 ± 0.02	19.26 ± 0.03	0.995
	$CH(CH_3)_2$	1.16	9	1.31 ± 0.05	19.24 ± 0.03	0.967
263	$CBPQT^{4+}$ α-*H*	8.89–9.24	5	3.01 ± 0.15	19.58 ± 0.04	0.922
	$CBPQT^{4+}$ β-*H*	8.12–8.44	5	3.04 ± 0.12	19.58 ± 0.03	0.942
	Stopper Ar-*H*	7.19 + 7.22	5	3.89 ± 0.14	19.45 ± 0.03	0.996
	OP-H_b	6.71	5	4.55 ± 0.66	19.37 ± 0.08	0.967
	SCH_2CH_3	1.55	5	4.12 ± 0.35	19.42 ± 0.05	0.993
	$C(CH_3)_3$	1.26	5	3.54 ± 0.03	19.50 ± 0.10	0.999
	$CH(CH_3)_2$	1.19	5	3.92 ± 0.09	19.45 ± 0.03	1.000
	$CBPQT^{4+}$ α-*H*	8.84	5	3.19 ± 0.13	19.56 ± 0.03	0.973
	Pyrrole-*H*	8.06	5	2.98 ± 0.47	19.59 ± 0.09	0.960
	OP-H_a	6.18	5	3.43 ± 0.57	19.52 ± 0.09	0.923
	NCH_2	4.55	5	3.78 ± 0.65	19.47 ± 0.09	0.916
	SCH_2CH_3	1.48	5	2.99 ± 0.32	19.59 ± 0.06	0.975
	OCH_2	1.42–1.46	5	2.57 ± 0.44	19.67 ± 0.09	0.988
	$C(CH_3)_3$	1.35	5	3.36 ± 0.04	19.53 ± 0.02	0.981
	$CH(CH_3)_2$	1.17	5	3.03 ± 0.08	19.58 ± 0.03	0.986
268	$CBPQT^{4+}$ α-*H*	8.90–9.20	5	8.73 ± 0.39	19.40 ± 0.03	0.928
	OP-H_b	6.72	5	9.21 ± 1.58	19.37 ± 0.09	0.942
	SCH_2CH_3	1.55	5	7.83 ± 0.82	19.46 ± 0.06	0.956
	$C(CH_3)_3$	1.26	5	5.88 ± 0.06	19.61 ± 0.02	0.992
	$CH(CH_3)_2$	1.19	5	6.42 ± 0.16	19.56 ± 0.03	0.989
	OCH_2	1.41–1.46	5	2.36 ± 0.35	20.10 ± 0.08	0.914
	$C(CH_3)_3$	1.35	5	3.08 ± 0.03	19.96 ± 0.02	0.940
	$CH(CH_3)_2$	1.17	5	2.40 ± 0.06	20.09 ± 0.03	0.929

[a]The errors are calculated using the method presented in Koumura *et al.*[S12] with ΔT = 0.3 K, I = 5% and t = 0.1 s.

Taking an average of the probes with $R^2 > 0.9$ at the four different temperatures, yielded a rate constant (k_1^{av}) for each temperature, which are listed for all temperatures in Table 2.

25 Derivation of expression for difference in Gibbs free energy of activation

The Gibbs free energy of activation $(\Delta G^{\ddagger})$[S12] is defined as.

$$\Delta G^{\ddagger} = -RT\ln\left(\frac{kh}{k_B T}\right)$$

where R is the gas constant (1.987×10^{-3} kcal K^{-1} mol^{-1}), T is the temperature, k is the rate constant, h is the Planck constant (1.38×10^{-23} J K^{-1}) and k_B is the Boltzmann constant (6.626×10^{-34} J s).

If k_{MPTTF} is the rate constant and $\Delta G^{\ddagger}(k_{MPTTF})$ is the Gibbs free energy of activation for the movement of $CBPQT^{4+}$ over an $MPTTF^{2+}$ dication and if k_{TTF} is the rate constant and $\Delta G^{\ddagger}(k_{TTF})$ is the Gibbs free energy of activation for the movement of $CBPQT^{4+}$ over a TTF^{2+} dication, the following expression for the difference in the Gibbs free energies of activation ($\Delta\Delta G^{\ddagger}$) can be derived:

$$\Delta\Delta G^{\ddagger} = \Delta G^{\ddagger}(k_{MPTTF}) - \Delta G^{\ddagger}(k_{TTF})$$

$$= -RT\ln\left(\frac{k_{MPTTF}h}{k_B T}\right) - \left(-RT\ln\left(\frac{k_{TTF}h}{k_B T}\right)\right)$$

$$= -RT\ln\left(\frac{k_{MPTTF}h}{k_B T}\right) + RT\ln\left(\frac{k_{TTF}h}{k_B T}\right)$$

$$= -RT\left(\ln\left(\frac{k_{MPTTF}h}{k_B T}\right) - \ln\left(\frac{k_{TTF}h}{k_B T}\right)\right)$$

$$= -RT\ln\left(\frac{\frac{k_{MPTTF}h}{k_B T}}{\frac{k_{TTF}h}{k_B T}}\right)$$

$$= -RT\ln\left(\frac{k_{MPTTF}}{k_{TTF}}\right)$$

This expression can be rearranged to:

$$\Delta\Delta G^{\ddagger} = -RT\ln\left(\frac{k_{MPTTF}}{k_{TTF}}\right) \Leftrightarrow \frac{k_{MPTTF}}{k_{TTF}} = \exp\left(-\frac{\Delta\Delta G^{\ddagger}}{RT}\right)$$

The percentage ratio of $CBPQT^{4+}$ moving over the $MPTTF^{2+}$ dication compared to the TTF^{2+} dication ($\%MPTTF^{2+}$) can be calculated in the following way, where it is exploited that $\frac{k_{TTF}}{k_{TTF}} = 1$.

$$\%MPTTF^{2+} = \frac{k_{MPTTF}}{k_{MPTTF} + k_{TTF}} \cdot 100 \Leftrightarrow \%MPTTF^{2+} = \frac{k_{MPTTF}}{k_{MPTTF} + k_{TTF}} \cdot \frac{k_{TTF}}{k_{TTF}} \cdot 100$$

$$\Leftrightarrow \%\mathrm{MPTTF}^{2+} = \frac{k_{\mathrm{MPTTF}} \cdot k_{\mathrm{TTF}}}{(k_{\mathrm{MPTTF}} + k_{\mathrm{TTF}})k_{\mathrm{TTF}}} \cdot 100$$

$$\Leftrightarrow \%\mathrm{MPTTF}^{2+} = \frac{k_{\mathrm{MPTTF}}}{k_{\mathrm{TTF}}} \cdot \frac{k_{\mathrm{TTF}}}{(k_{\mathrm{MPTTF}} + k_{\mathrm{TTF}})} \cdot 100$$

$$\Leftrightarrow \%\mathrm{MPTTF}^{2+} = \frac{\frac{k_{\mathrm{MPTTF}}}{k_{\mathrm{TTF}}}}{\frac{k_{\mathrm{MPTTF}} + k_{\mathrm{TTF}}}{k_{\mathrm{TTF}}}} \cdot 100$$

$$\Leftrightarrow \%\mathrm{MPTTF}^{2+} = \frac{\frac{k_{\mathrm{MPTTF}}}{k_{\mathrm{TTF}}}}{\frac{k_{\mathrm{MPTTF}}}{k_{\mathrm{TTF}}} + \frac{k_{\mathrm{TTF}}}{k_{\mathrm{TTF}}}} \cdot 100$$

$$\Leftrightarrow \%\mathrm{MPTTF}^{2+} = \frac{\frac{k_{\mathrm{MPTTF}}}{k_{\mathrm{TTF}}}}{\frac{k_{\mathrm{MPTTF}}}{k_{\mathrm{TTF}}} + 1} \cdot 100$$

The ratio of $CBPQT^{4+}$ moving over the TTF^{2+} dication ($\%TTF^{2+}$) can be calculated in a similar way, or by using the following connection between $\%MPTTF^{2+}$ and $\%TTF^{2+}$.

$$\%\mathrm{TTF}^{2+} = 100 - \%\mathrm{MPTTF}^{2+}$$

Therefore, the ratios of $CBPQT^{4+}$ moving over the $MPTTF^{2+}$ dication and the TTF^{2+} dication can be calculated using either $\Delta\Delta G^{\ddagger}$ or the ratio of the rate constants $\frac{k_{\mathrm{MPTTF}}}{k_{\mathrm{TTF}}}$ using the following equations.

$$\frac{k_{\mathrm{MPTTF}}}{k_{\mathrm{TTF}}} = \exp\left(-\frac{\Delta\Delta G^{\ddagger}}{RT}\right) \text{ and } \%\mathrm{MPTTF}^{2+} = \frac{\frac{k_{\mathrm{MPTTF}}}{k_{\mathrm{TTF}}}}{\frac{k_{\mathrm{MPTTF}}}{k_{\mathrm{TTF}}} + 1} \cdot 100$$

26 References

S1 L. J. O'Driscoll, S. S. Andersen, M. V. Solano, D. Bendixen, M. Jensen, T. Duedal, J. Lycoops, C. Van Der Pol, R. E. Sørensen, K. R. Larsen, K. Myntman, C. Henriksen, S. W. Hansen and J. O. Jeppesen, *Beilstein J. Org. Chem.*, 2015, **11**, 1112–1122.

S2 M. S. Neumann, A. F. Smith, S. K. Jensen, R. Frederiksen, M. L. Skavenborg and J. O. Jeppesen, *Chem. Commun.*, 2023, **59**, 6335–6338.

S3 R. Crossley, Z. Goolamali, J. J. Gosper and P. G. Sammes, *J. Chem. Soc., Perkin Trans. 2*, 1994, 513–520.

S4 J. Becher, J. Lau, P. Leriche, P. Mørk and N. Svenstrup, *J. Chem. Soc., Chem. Commun.*, 1994, 2715–2716.

S5 S. S. Andersen, A. I. Share, B. L. C. Poulsen, M. Kørner, T. Duedal, C. R. Benson, S. W. Hansen, J. O. Jeppesen and A. H. Flood, *J. Am. Chem. Soc.*, 2014, **136**, 6373–6384.

S6 P. L. Anelli, P. R. Ashton, R. Ballardini, V. Balzani, M. Delgado, M. T. Gandolfi, T. T. Goodnow, A. E. Kaifer, D. Philp, M. Pietraszkiewicz, L. Prodi, M. V. Reddington, A. M. Z. Slawin, N. Spencer, J. F. Stoddart, C. Vicent and D. J. Williams, *J. Am. Chem. Soc.*, 1992, **114**, 193–218.

S7 J. W. Choi, A. H. Flood, D. W. Steuerman, S. Nygaard, A. B. Braunschweig, N. N. P. Moonen, B. W. Laursen, Y. Luo, E. Deionno, A. J. Peters, J. O. Jeppesen, K. Xu, J. F. Stoddart and J. R. Heath, *Chem. − Eur. J.*, 2006, **12**, 261–279.

S8 G. R. Fulmer, A. J. M. Miller, N. H. Sherden, H. E. Gottlieb, A. Nudelman, B. M. Stoltz, J. E. Bercaw and K. I. Goldberg, *Organometallics*, 2010, **29**, 2176–2179.

S9 Signals are missing or coinciding with other signals.

S10 M. Jensen, R. Kristensen, S. S. Andersen, D. Bendixen and J. O. Jeppesen, *Chem. − Eur. J.*, 2020, **26**, 6165–6175.

S11 The $\Delta G^{\ddagger}$ values were calculated using the Eyring relationship $\Delta G^{\ddagger} = RT \ln(kh/k_B T)$, where R is the gas constant, T is the absolute temperature, k is the rate constant, h is the Planck constant and k_B is the Boltzmann constant.

S12 N. Koumura, E. M. Geertsema, M. B. Van Gelder, A. Meetsma and B. L. Feringa, *J. Am. Chem. Soc.*, 2002, **124**, 5037–5051.